DIURNAL AND SEASONAL VARIABILITY OF URANUS' MAGNETOSPHERE UNDER DIFFERENT IMF

A Dissertation
Presented to
The Academic Faculty

by

Xin Cao

In Partial Fulfillment
of the Requirements for the Degree
Doctor of Philosophy in the
School of Earth and Atmospheric Sciences

Georgia Institute of Technology
December 2018

DIURNAL AND SEASONAL VARIABILITY OF URANUS' MAGNETOSPHERE UNDER DIFFERENT IMF

Approved by:

Dr. Carol Paty, Advisor
School of Earth and Atmospheric Sciences
Georgia Institute of Technology

Dr. Paul Steffes
School of Electrical and Computer Engineering
Georgia Institute of Technology

Dr. Zhigang Peng
School of Earth and Atmospheric Sciences
Georgia Institute of Technology

Dr. Mitchell Walker
Daniel Guggenheim School of Aerospace Engineering
Georgia Institute of Technology

Dr. James Wray
School of Earth and Atmospheric Sciences
Georgia Institute of Technology

Date Approved: October 19th, 2018

To my families and endlessness of our human's curiosity

ACKNOWLEDGEMENTS

I would like to thank my advisor Dr. Carol Paty. Without her support and encouragement, I would not finish my exciting research during my PhD studies. Her broad insight, deep understanding and rich experience in the field of planetary space physics has inspired me to discover and challenge the interesting scientific problems throughout my doctoral period. Her abundant patience and continuous encouragement has motivated me to move on no matter how difficult I encountered a problem in my research.

I also would like to thank my colleagues in my group: Ashok Rajendar, Jeremy Riousset, John Hale. They did give me a great help during my PhD period. I really enjoyed the time when we discussed scientific problems and coding problems. I would like to thank my good friends in planetary science and geophysics group as well: Lujendra Ojha, Mary Beth Wilhelm, Dongdong Yao, Zefeng Li and Xiaofeng Meng.

I would like to thank my defense committee: Dr. Zhigang Peng, Dr. James Wray, Dr. Paul Steffes and Dr. Mitchell Walker, for their kind support and insightful comments. Their professional advices benefited me for my academic career.

Finally, I would like to express my deep gratitude to my mother, father and all of my families including my grandma and grandpa, my uncles and aunts. They taught me a lot in my life. They always support me to pursue my career. Especially thank my mom for her sacrifice during my growing up. I wish I could share my PhD degree with her.

TABLE OF CONTENTS

LIST OF FIGURES

SUMMARY

The magnetosphere of Uranus is far from well known since there was only one fly-by measurement in history. In order to study the magnetosphere and its coupling mechanism with the solar wind, we used our multifluid magnetohydrodynamics (MHD) model [Cao and Paty, 2017] to successfully simulate the variation of the global magnetosphere of Uranus and have predicted potential favorable reconnection locations. We investigated the existence of a "switch-like" magnetosphere at Uranus for both equinox and solstice seasons, where the planetary rotation drives the interchange between an open magnetosphere and a closed magnetosphere each Uranus day. This periodic reconnection is predicted to occur upstream of the magnetopause, with a frequency that corresponds to the planetary rotation (once per 17.24 hours). The locations of the bow shock and magnetopause in our model are validated against measurements made by Voyager 2. In examining the evolution of the magnetic field configuration along with that of high plasma beta regions, which in combination indicate where the system is favorable for reconnection, we found that the occurrence of reconnection is highly dependent on the rotation of the planetary magnetic field in both equinox and solstice seasons. These periodic reconnection events in our simulation support the hypothesis of a periodic "switch-like" magnetosphere at Uranus during different seasons. We then investigated the diurnal and seasonal variations of the magnetopause boundary under different Interplanetary Magnetic Field (IMF) orientations, combined with Voyager 2's measurement. We quantitatively analyzed the characteristics and variability of Uranus' magnetopause and cusp in terms of the subsolar's standoff distance, the flaring parameter and the cusp indentation, which give us an initial

intuition of the asymmetric structure of the magnetopause. Our results show that the asymmetry of the magnetopause is highly dependent on the rotation of Uranus under specific IMF orientations. The shape of the magnetopause is also affected by the off-centered dipole moment. Our model can be applied to other planets with different magnetic geometries, such as the exoplanets and the Neptune-Triton system.

CHAPTER 1. INTRODUCTION

1.1 Planetary magnetospheres

1.1.1 Why do we study magnetospheres?

A magnetosphere is a spatial cavity that is formed by the interaction between the magnetic field of a planet and the high-speed magnetic solar wind, which is full of energetic and charged hot particles, such as protons, helium ions, electrons and other heavy ions. The magnetosphere is very important for the habitability of a planet because it provides a natural umbrella that protects the planet from the stellar wind. Without the protection of a magnetosphere, solar wind radiation would directly impact the surface and erode the atmosphere away from the planet, making life exposed to high radiation.

Earth is very lucky to have such a strong and stable magnetosphere to resist the solar wind. Venus, a planet in our solar system that is closer to the Sun than Earth, has no magnetosphere produced by an intrinsic dynamo. Therefore, it does not have such a protection from the solar radiation, compared with the Earth. Mercury, another planet that orbits the sun and is even closer to the Sun than Venus, has a global magnetosphere like that of Earth. However, the magnetic field strength on its surface is much lower (approximately 1%) than that on the surface of the Earth. As measured by the MESSENGER spacecraft, the magnetopause standoff distance, which is a measurement of the strength of the resistance of a planet's magnetosphere against the solar wind, is much closer to Mercury compared with that for Earth, and Mercury has a much smaller magnetosphere. Thus, its resistance to the solar wind is much weaker than that of Earth.

Mars, which is the most similar to Earth in our solar system, holds the possibility of colonization in the future and is thus fascinating to us. Unfortunately, Mars has not been found to have a global magnetosphere like Earth, even though there is solid evidence that it did hold a global magnetosphere at billions of years ago. However, the magnetic field faded over time. Without the global protection of a magnetosphere, the surface environment on Mars is exposed to solar wind radiation, making it less habitable than the Earth surface.

1.1.2 How are magnetospheres formed?

A planetary magnetosphere is formed by the interaction between the high-speed solar wind (typically supersonic) and the planetary magnetic field. In detail, the solar wind is a continuous high-speed plasma flow that is composed of primarily protons and electrons escaping from the corona of the Sun. The speed of the solar wind could reach up to hundreds of kilometers per second near the Earth. The solar wind plasma is embedded with a magnetic field, which means it carries a magnetic field with it because of the frozen-in effect [Baumjohann et al., 1996] of the high conducting plasma of the solar wind. Thus, the solar wind plasma and the magnetic field (also known as the Interplanetary Magnetic Field or IMF) are coupled with each other as they move together from the surface of the Sun outwards to orbiting planets.

If a planet is unmagnetized (i.e., no intrinsic magnetic field), which means it has no intrinsic magnetic field, the highly energetic charged particles in the solar wind can directly impact the atmosphere or even penetrate to the surface of the planet. A recent investigation on Mars found that the solar wind results in significant ions escaping from its atmosphere

[Dong et al., 2014]. If a planet is magnetized (i.e., with an intrinsic magnetic field), which means it has an intrinsic magnetic field, most of the highly energetic charged particles in the solar wind can be deflected by the planetary magnetic field and therefore can not easily penetrate into the atmosphere or to the surface of the planet, as is the case for Earth, Jupiter and Saturn.

When the solar wind starts to interact with a magnetized planet upstream, it slows from supersonic down to subsonic due to the obstructing planetary magnetic field, forming a bow shock structure (Figure 1.1). Across this region, the solar wind plasma is thermalized and densified, which is called magnetosheath. To keep track of the plasma flow downstream, the magnetopause boundary deflects most of the upstream plasma by balancing the kinetic pressure of the solar wind and the magnetic pressure of the planet. The solar wind generally compresses the dayside magnetic field of the planet and stretches the nightside field in the region called magnetotail [Baumjohann et al., 1996]. Ignoring the high order terms of the magnetic moment, the magnetic field close to the surface of the planet can be roughly considered as a dipole field. This is because the spatial size that we study is large enough, and the high order terms can be neglected.

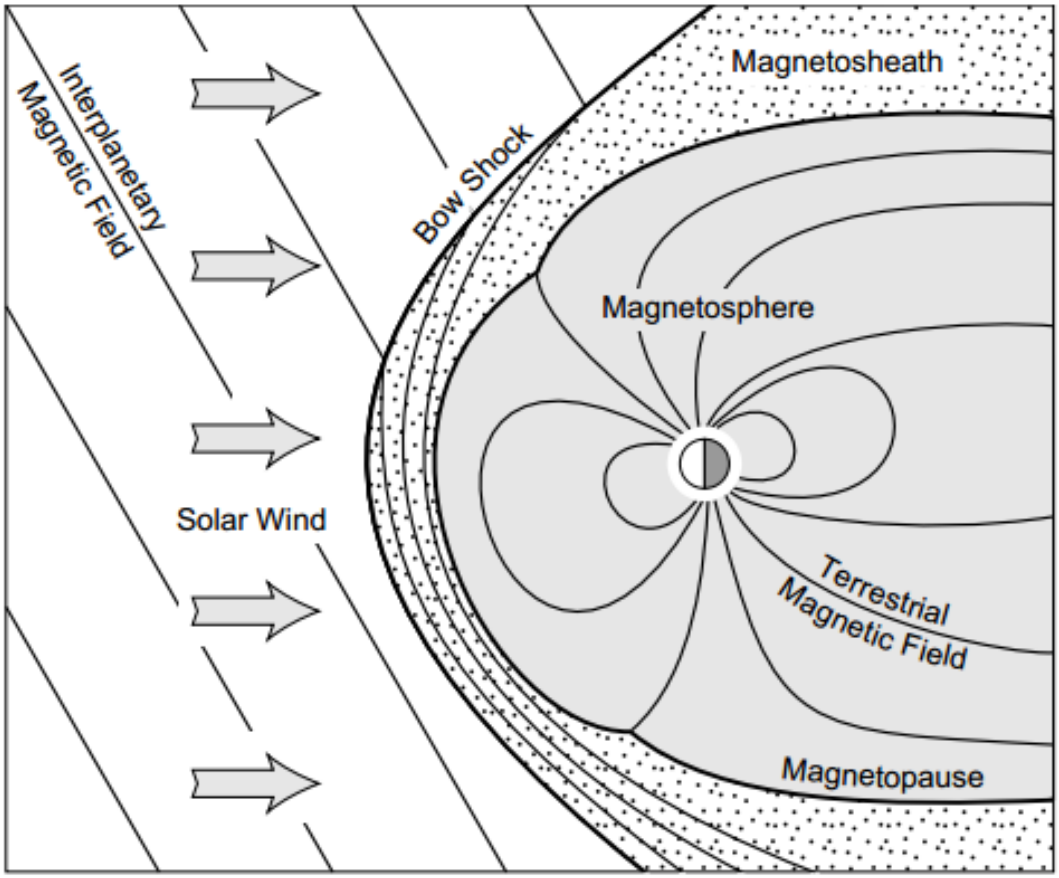

Figure 1.1 The configuration of Earth's magnetosphere. The upstream solar wind moves from the left side of this figure (Baumjohann et al., 1996).

1.1.3 What is the morphology of the magnetosphere of Uranus?

Uranus is an ice giant planet orbiting 19 Astronomical Unit (AU) from the Sun with a radius R_U=25,484 km, which is four times larger than the radius of Earth. The magnetic dipole moment is approximately fifty times that of Earth with an equatorial surface field strength of 23 μT [Russell, 1993], and its orbital period is approximately 84 years. Voyager 2 data have shown that the obliquity of the rotation axis of Uranus is approximately 98º and a large angle (59º) exists between the rotation axis and the magnetic axis. In addition, the magnetic dipole of Uranus is shifted by 1/3 R_U southwards from its geometric center

(Figure 1.2). These characteristics illustrate the uniqueness of the magnetic configuration of the ice giants, indicating that they have a different planetary dynamo mechanism from that of the other major planets. Where and how the magnetic field is generated is still an important question to answer [Hofstadter].

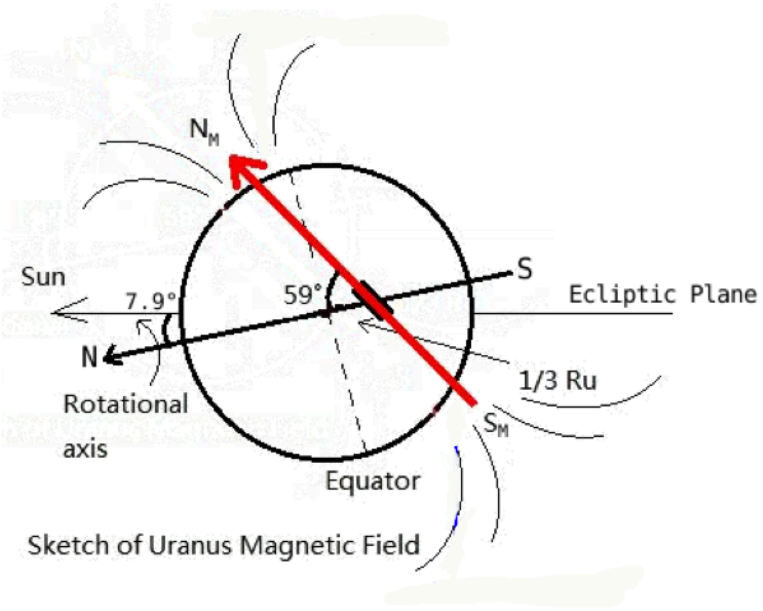

Figure 1.2 The rotational and magnetic configuration of Uranus.

The rotational and magnetic morphology of Uranus is extremely unusual as mentioned above. All of these morphological characteristics of Uranus under its rapid rotation (17.24 hours per Uranus day) results in an asymmetrically dynamic magnetosphere. Considering the long orbital period, the magnetosphere of Uranus must experience significant seasonal variations over the course of its orbit. Because Uranus is much further from the Sun than the Earth, the density of the solar wind is lower than that of the solar wind density near the Earth. Voyager 2 measurements show an approximate mass density of 0.05 amu/cm^3, which is in agreement with the density decreasing roughly

with a square increase in the distance. The mean solar wind velocity is approximately 450 km/s, and the temperature of the solar wind plasma is approximately 4.7 eV (54,541 K) [Tóth et al., 2004].

I am interested in studying the seasonal variations of the magnetosphere of Uranus because we know that the planet's magnetosphere significantly changes every 21 years from solstice to equinox to the next solstice. Twenty-one years after the Voyager 2 fly-by, Uranus approached its autumnal equinox, and its rotation axis was perpendicular to the line connecting the Sun and Uranus. After another 21 years, in 2028, Uranus will approach its first winter solstice since 1986, and its rotation axis will approximately point away from the Sun. When Uranus approaches its vernal equinox in 2049, it rotational axis will be parallel to the line towards the Sun; however, its positive direction will be opposite that of 2007. From a theoretic analysis, we can expect that the magnetic pattern of the magnetotail looks like an anticlockwise rotating helix during the summer solstice (1986) and looks like a clockwise rotating helix during the winter solstice (2028). In contrast, the evolution of the magnetic dipole of Uranus looks like a kayak paddle rowing downstream during the autumnal equinox (2007) and looks like a kayak paddle rowing upstream during the vernal equinox (2049). Each phase of its magnetosphere in the orbit has a totally unique magnetospheric configuration, and a different coupling process between the solar wind and magnetic dipole is expected. Because the orbital period of Uranus is so long that each phase can be expected to become stable if the solar wind has no large turbulence during that time, this is definitely a good opportunity to perform a comparative study of the similarities and differences of the four extreme magnetospheric morphologies of Uranus and the other ice giant, Neptune.

1.1.4 How do the dynamics in a magnetosphere vary?

The magnetospheric dynamics are complex because of the solar wind–magnetosphere–ionosphere coupling. For example, in the region close to the Earth, the strong magnetic field co-rotates with the planet and carries frozen plasma, which undergoes corotational dynamics. In the outer magnetospheric region, the dynamics are dominated by convection. The convection of Earth's magnetosphere is driven by the solar wind. Especially in southward IMF conditions, the dayside reconnection occurs at the sub-solar point at the magnetopause because the IMF is antiparallel to the terrestrial magnetic field. The convection driven by the solar wind starts from the dayside reconnection and opens the dayside terrestrial field lines, transporting the plasma flow to the nightside. At the nightside, the convection moves the plasma flow back sunward through the tail current sheet reconnection and finally transports it back to the dayside. The corresponding dayside–nightside–dayside repeated transportation is called the Dungey cycle [Dungey, 1961].

The Dungey cycle describes how the plasma flow convects in the magnetosphere, which is driven by the dayside and nightside reconnection. If the dayside reconnection rate equals that at the nightside, the convection approaches a stable status. However, it is more frequent for the convection to be unstable because the two side reconnection rates are rarely equal to each other [Zhang et al., 2015]. The unequal reconnection rates between dayside and nightside trigger a disturbance of plasma energy in the magnetosphere, which is called a substorm. A substorm event can result in aurora emission at high latitude. Therefore, we can investigate the occurrence of substorm events by observing aurora emissions.

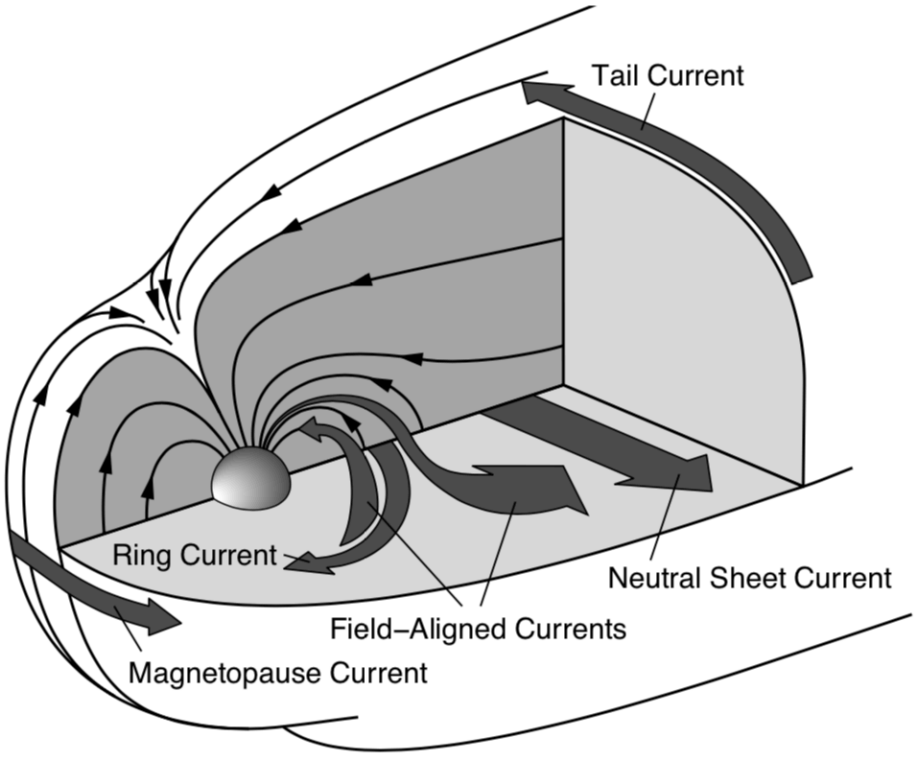

Figure 1.3 The current system of the magnetosphere (Baumjohann et al., 1996).

Based on the theory of single particle motion, the drift motions of different charged particles may occur in different directions. Therefore, a current system in the magnetosphere forms. There are different regional electric currents in the system. They include the magnetopause current, ring current, field-aligned current, neutral sheet current, and tail current [Baumjohann et al., 1996] as shown in Figure 1.3.

1.1.5 Comparative planetology: Earth, Jupiter, Saturn, and Uranus

In our solar system, most of the planets have an intrinsic magnetic field. For example, Earth, Jupiter, Saturn, Uranus, and Neptune have relative large-scale

magnetospheres. Mercury has an intrinsic field with a much smaller magnitude. Thus, its magnetosphere is much smaller than those of other planets.

The obliquity of Earth's rotational axis is approximately 23.5°, and the dipole tilt has changed from 11.7° to 10.5° in the last few decades [Cnossen et al., 2012]. Compared with the Earth, Jupiter has an obliquity of 3° [Mosqueira et al., 2006] and a dipole tilt of approximately 10° [Russell et al., 2010]. Saturn has an obliquity of 26.7° [Arridge et al., 2008] and a very small dipole tilt [Russell et al., 2010]. The rotational periods of the Earth, Jupiter, and Saturn are approximately 23.9, 10, and 10.5 hours, respectively. Compared to Uranus, the magnetic tilt angle of Earth and the gas giant planets are much smaller. Therefore, their magnetospheres are to some extent similar to that of Earth. For example, their northern magnetic poles are always oriented towards north or south.

Uranus, the seventh planet in our solar system sorted by the distances from the Sun, has a strong global magnetosphere. The average magnetic strength at the surface is 23 μT, which is almost the same as that at the surface of the Earth. There are several differences between Uranus and Earth. First, Uranus has a very high obliquity. Its rotational axis is approximately 97.9° away from the northward direction. From the side view in space, Uranus looks to be lying on the ecliptic plane with a rapid rotational period of 17.24 h per Uranus day. Second, the magnetic axis of Uranus is largely tilted (at approximately 59°) away from the rotational axis compared to 11° for Earth. This is the largest magnetic tilted angle in our solar system. Finally, the magnetic dipole moment of Uranus is not located in the center of the planet like that of Earth. Instead, it is off-centered and shifted 1/3 Uranus radii towards the geometric southern pole. Because Uranus has these characteristics, an

extremely dynamic and asymmetric magnetosphere is formed by the interaction with the upstream solar wind.

As expected, the magnetospheres of the gas giants are different from that of Earth. One of the most significant differences is that there is another convection existed in the magnetospheres of the gas giants. This convection is called the Vasyliunas cycle as proposed by Vasyliunas [1983]. The Vasyliunas cycle describes the convection of the internally driven magnetosphere due to the fast rotation of the planet and the corotation of the plasma with the planet. The fast rotation exerts a strong centrifugal stress on the internal plasma, which is transported from the internal region to the magnetotail through the local reconnection. Therefore, the fast rotation of the planet plays an important role in the convection inside the magnetosphere.

The convection of the magnetosphere of Uranus is still unknown. The solar wind drives the magnetospheric convection of Uranus; however the corotation effect on the convection is not negligible [Vasyliunas, 1986; Ye and Hill, 1994] because the rotational period of Uranus is relative fast (between that of Earth and those of Jupiter and Saturn). Moreover, the dipole moment of the magnetic field of Uranus is off-centered and shifted towards the geometric south pole. This off-centered dipole results in a shifted difference in the two magnetic poles combined with a largely tilted magnetic axis. Because of this magnetic structure, the aurora emission on Uranus can be observed at lower latitudes.

1.1.6 What implications does Uranus provide for exoplanets and magnetic reversal?

Studying Uranus is not only important for investigating the formation and evolution of our solar system. It is also important for us to know more about a large number of

exoplanets in our universe. The Kepler telescope found thousands of exoplanets exist in our galaxy. The majority of the exoplanets are Uranus/Neptune-sized or sub-Uranus/sub-Neptune-sized planets. How the complex magnetospheres, such as that of Uranus, shield stellar radiation from their atmospheres or surfaces is of key importance for studying the habitability of these newly discovered worlds. How potential life originates and evolves in such an environment is unknown, which is not possible in the natural environment of our Earth. Therefore, the magnetosphere of Uranus is the best natural laboratory for learning about the habitability of distant exoplanetary worlds. For example, we might expect that the polar outflow of ions from the ionosphere is different from the process on Earth because a Uranus-like magnetosphere has a periodic open-closed structure, which can result in a much more dynamical and asymmetric convection in the magnetosphere [Cao and Paty, 2017].

Another implication is that we can investigate what the magnetosphere of Earth may experience during its magnetic reversal when the magnetic pole would switch its position. This is somewhat similar to the switch of the magnetic poles of Uranus via its rotation with a large magnetic tilt angle. Although the time scale of Earth's magnetic reversal is much longer than that of the rotation or Uranus, it can still provide some insights on the physical processes during the switch of magnetic pole position.

1.2 Questions regarding the current state of the science on the magnetosphere of Uranus

Before Voyager 2 flew by Uranus and Neptune, we had little knowledge of the magnetic field morphologies of these ice giants. Using the Voyager 2 measurements,

Behannon et al. [1987] found that the magnetosphere of Uranus was extremely dynamic. One of most important characteristics of the magnetosphere of Uranus is its twisted magnetotail, as mentioned previously. For other planets such as Earth or Jupiter, there is usually a relatively thin and flat current sheet in the tail region where the tail reconnection occurs and E×B drift transports charged particles planetward (E×B drift is the drift motion of charged particles dominated by both the electric and magnetic fields). In contrast, at Uranus, Voyager 2 measured a twisted current sheet, forming a helix-like configuration. This difference leads to many questions that we never encountered regarding the magnetosphere of Earth. Here is a list of four questions:

(1) Given the complex rotational and magnetic geometry, how does reconnection vary and evolve with the rapid rotation of Uranus?

(2) Where is the magnetosphere stable for reconnection during rotation? How does the reconnection affect the configuration of the magnetosphere of Uranus (e.g., the global structure, boundaries, and current sheet)?

(3) How does the magnetopause evolve with rotation under different IMF orientations?

(4) How should we investigate magnetopause characteristics, such as cusp indentation and flaring parameters, as they relate to the seasons and the IMF?

Based on these considerations, the unique morphology of the magnetosphere of Uranus is expected to result in considerably different magnetospheric dynamics from what we have observed previously. Therefore, the magnetosphere of Uranus is one of the most

mysterious natural phenomena in our solar system. Studying it will improve our understanding of magnetospheric behavior.

In this dissertation, I will address all of the above four questions. NASA supports the development space science techniques that focus on numerical simulation, modeling, analysis and interpretation of space data [NASA, 2010]. My research aims to develop a set of numerical simulation and modeling methods to meet this goal. Additionally, the Heliophysics Research Program of NASA "supports investigations of the origin and behavior of the solar wind, energetic particles, and magnetic fields in the heliosphere and their interaction with the Earth and other planets..." [NASA, 2010]. Our objective is to study the dynamics of the solar wind, energetic particles and magnetic fields in magnetospheres of ice giant planets in our solar system using multifluid MHD (magnetohydrodynamics) simulations. As outlined in the Vision and Voyages for Planetary Science in the Decade 2013-2022 [National Academy of Sciences, 2011], "The third highest priority Flagship mission is the Uranus Orbiter and Probe mission. The committee carefully investigated missions to both ice giants, Uranus and Neptune. It should be initiated in the decade 2013-2022 even if both MAX-C and JEO take place" to seek to answer "How do the giant planets serve as laboratories to understand Earth, the solar system, and extrasolar planetary systems?" [National Academy of Sciences, 2011]. My research on the extreme dynamic magnetic structure of ice giant planets is definitely expected to be an ideal laboratory tool.

1.3 How much do we know about the magnetosphere of Uranus?

We did not know about the magnetic and rotational geometries of Uranus until the Voyager 2 spacecraft flew by the planet in 1986. The solar wind drives the magnetospheric convection of the magnetosphere of Uranus, although the rotation-driven dynamics are not negligible [Vasyliunas, 1986; Ye and Hill, 1994]. Connerney [1993] found that the aurora appears much closer to the geometric equator than to the poles. Lamy et al. [2012] observed the UV aurora of Uranus via the Hubble Space Telescope and confirmed the assumed latitudinal distribution of auroras. Behannon et al. [1987] used Voyager 2's data to measure the magnetotail lobes of Uranus, which have an average pitch angle for the helical twist of approximately 5.5° with a curved plasma sheet. Some empirical models described this asymmetry in a tilted magnetosphere. For instance, Schulz and McNab [1996] used a model to simulate that different structures in the plasma sheet result from different tilt angles of a magnetic axis. Masters [2014] used an analytical model and found that geometries that favor reconnection are highly related to the planetary rotation. Tóth et al. [2004] used a numerical model of the magnetosphere of Uranus to investigate the twisted magnetotail during the solstice season, assuming that the IMF is zero. However, it is still not known how the magnetosphere of Uranus varies with the planetary rotation and with different seasons under different IMF conditions, how the dayside reconnection affects the global magnetosphere, or how the magnetospheric boundary responds to the IMF orientation during different seasons. These issues were the focus of this dissertation research.

1.4 Scope of this dissertation

The objective of this dissertation was to establish a new magnetospheric model of Uranus that can be extended for the other ice giants via multifluid MHD simulations. I used data from Voyager 2's encounter and observations from the Hubble Space Telescope

(HST) to validate our model. I studied the magnetospheric morphology of Uranus, which is currently poorly understood, including where and how the twisted magnetotail of Uranus evolves, what factors affect this structure and how the reconnections drive the global structure of the Uranus magnetosphere.

Based on the establishment of the typical seasonal magnetospheres of Uranus, I focused on the differences between each season. The 1986 and 2007 auroras, which are the footprints of the precipitating plasma particle distributions and magnetic structure, had different patterns and intensities [Lamy et al., 2012]. The variation in the auroral morphology indicates that the transition from solstice to equinox on Uranus results from unusual magnetospheric dynamics. However, we cannot provide an image that describes the differences unless simulations are performed because a MHD simulation focusing specifically on the diurnal and seasonal variations in the magnetosphere of Uranus was deficient. Thus, the locations of magnetic reconnection may be distinct and may change as Uranus orbits the Sun. The Dungey cycle and global plasma convection may be strongly affected or even severely disturbed by the change in the magnetic reconnection rate. Uranus provides scientists an idea natural laboratory to study the space plasma environment, which is completely different from the space plasma environment at the Earth. By developing a deeper understanding of Uranus, I have more confidence to analogically study the magnetospheric configurations of exoplanets.

In this dissertation, I first discuss the measurements and observations from Voyager 2, the Hubble Space Telescope and ground-based detection of the magnetosphere of Uranus. I also review the previous theoretical studies, including the MHD simulations. Second, I will demonstrate my recent work on the diurnal and seasonal variability of the

magnetosphere of Uranus using the multifluid MHD model. I will discuss how the reconnection on the magnetopause dominates the global structure of the magnetosphere of Uranus. Third, I will discuss more details of the magnetosphere: the magnetopause. Since the magnetopause is the boundary where the interaction with the solar wind occurs, studying the diurnal and seasonal variations of the magnetopause can provide more information about how the complex magnetosphere forms. Finally, I will discuss future work based on our numerical model, which can be applied to the study of the Neptune/Triton system and exoplanets.

CHAPTER 2. OBSERVATIONS AND PREVIOUS THEORETICAL STUDIES

2.1 Observations from Voyager 2

Voyager 2 is the only spacecraft that has flown by Uranus, which occurred in 1986. The structure of the magnetic field of Uranus was not known until Voyager 2's measurements. Now, we know that Uranus has a large tilt angle between the magnetic axis and the rotation axis with a high obliquity of the rotation axis, which is 97.9° from the north direction. These large angles of Uranus make it unique in our solar system. Because Voyager 2 flew through the inner magnetosphere of Uranus, it took measurements that showed that the inner magnetosphere is close to the dipole field as shown in Figure 2.1 [Behannon et al., 1987]. When the spacecraft flew into the outer magnetosphere, the magnetic field became less dipole-like. The vertical dashed lines in the figure represent the crossing events of the current sheet. The subfigure in the upper right side shows the trajectory of Voyager 2 flying by the magnetosphere of Uranus. Voyager 2 measured that the current sheet had transient expansions and contractions, and these temporal variations may have been produced by a substorm in the magnetosphere [Behannon et al., 1987].

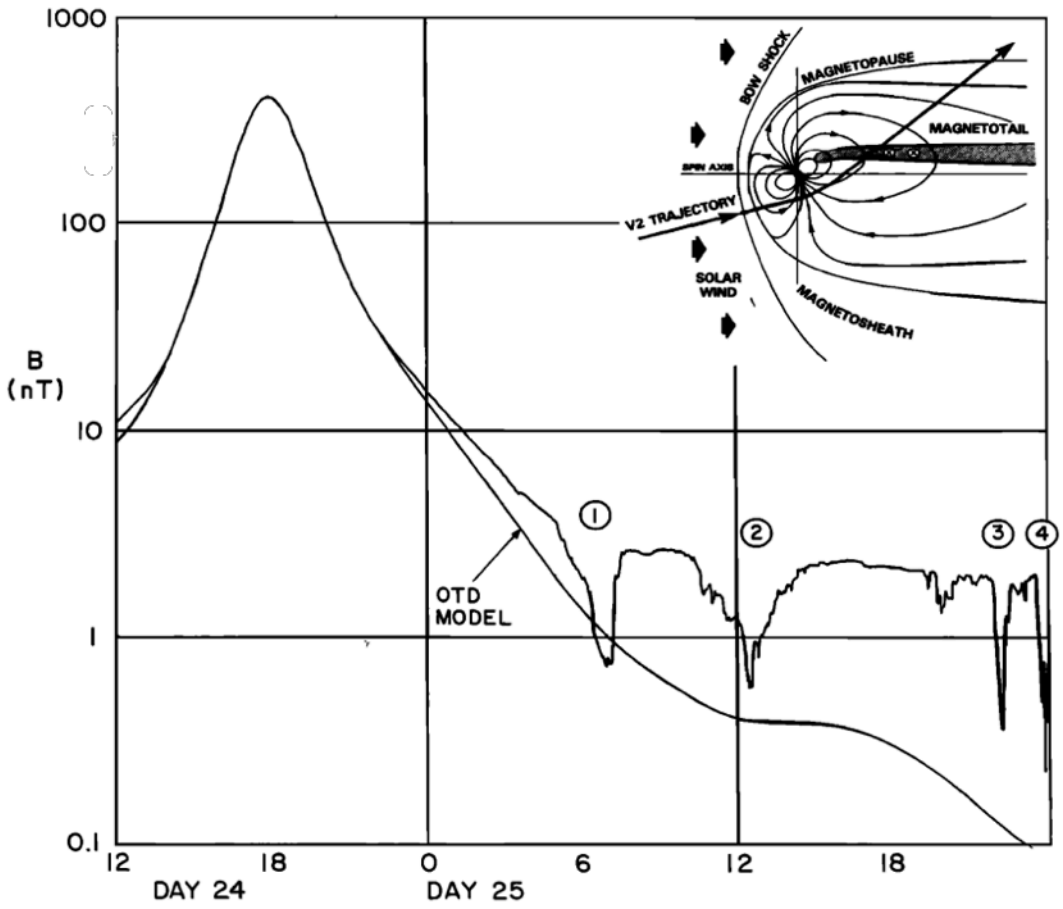

Figure 2.1 The magnetic field strength measured by Voyager 2's fly-by in 1986, compared with an offset tilted dipole field (OTD) (Behannon et al., 1987).

Voyager 2 also measured the plasma wave activities during its fly-by of the magnetosphere of Uranus. Figure 2.2 shows the plasma wave activities detected during the trajectory of the spacecraft. Based on that data, some local structures, such as the current sheet and other boundary layers, were identified. The plasma waves in the southern hemisphere were found to be asymmetric, which may be due to the off-centered and tilted dipole moment, and the magnetotail of Uranus has a very dynamic manner [Kurth et al., 1989].

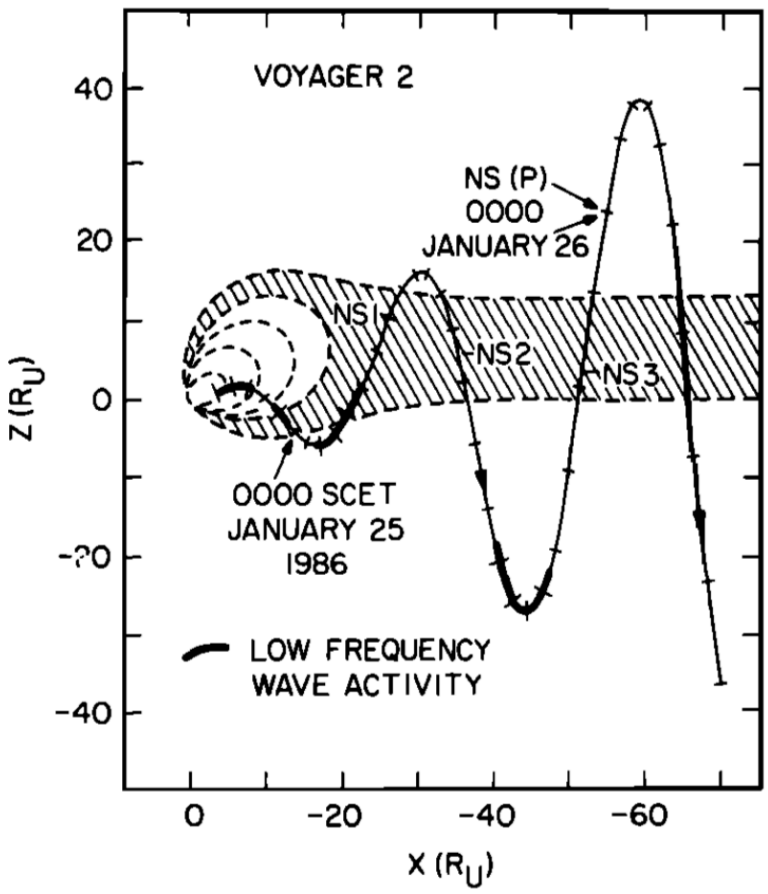

Figure 2.2 Plasma wave activities in the trajectory of Voyager 2 in the magnetosphere of Urnaus (Kurth et al., 1989).

Desch et al. [1986] used the Voyager 2 fly-by detection at Uranus to derive an intrinsic rotation period of 17.24±0.01 hours. Bridge et al. [1986] analyzed the Voyager 2 data to investigate the plasma density and temperature near Uranus and found that the Uranian moons do not appear to be a significant plasma source. Richard et al. [1987] analyzed the Voyager 2 data regarding the plasma ion density and temperature to calculate the flux tube particle and energy content and explained the sharp boundaries in the high-energy (at approximately 1 keV) plasma population. Krimigis et al. [1986] used data from the low-energy charged particle (LECP) instrument on Voyager 2 to analyze the low-

energy ions and electrons to map the energy range of charged particles in the magnetosphere of Uranus. A plasma residence time during convection in the magnetosphere was identified by Belcher et al. [1991]. Broadfoot et al. [1986] studied the atmosphere of Uranus and analyzed the relationship of aurora emission and molecular hydrogen distribution. Behannon et al. [1987] used an offset tilted dipole model to simulate the inner magnetosphere and magnetotail after Voyager 2 flew by Uranus. They found that the inner magnetosphere of Uranus is close to the magnetic dipole field but the magnetotail is not. He also analyzed the data when Voyager 2 crossed the current sheet and found that there are either transient expansions and contractions of the sheet or large perturbational torquing motions of the tail [Behannon et al., 1987]. Herbert et al. studied the relationship between the aurora-exciting energy and plasma convection in the magnetosphere of Uranus [Herbert et al., 1994]. He also used a method combined with the aurora to improve the resolution of the magnetic field measurements from Voyager 2 [Herbert, 2009].

2.2 Observations from the Hubble Space Telescope and ground-based telescopes

Since there are limitations to directly measuring the magnetosphere of Uranus, practical and efficient methods include ground-based or space-based telescope observations. One of the most powerful telescopes is the Hubble Space Telescope. Lamy et al. [2012] used the Hubble Space Telescope to observe aurorae emissions on the surface of Uranus, as shown by the white spots in Figure 2.3. The aurorae emissions were located at latitudes close to the magnetic poles, which probably corresponds to the injection of charged particles from the related cusp regions.

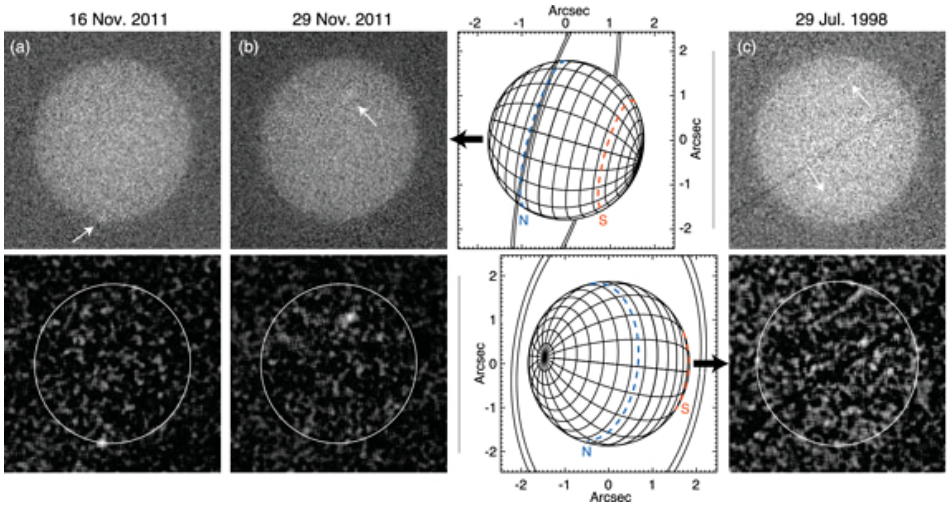

Figure 2.3 The images from Hubble Space Telescope. The images (a) and (b) were observed in 2011 and (c) was in 1998 (Lamy et al., 2012).

When Uranus orbited past the equinox season, Lamy et al. [2017] used the Hubble Space Telescope again to investigate the aurorae emission in 2012 and at a different time in 2014. They found that the aurorae emissions appeared in the southern latitude and lasted for a time scale of tens of minutes with variations of a few seconds, as shown in Figure 2.4. The authors suggested that the observed pulsed cusp aurorae emission may be caused by compressions of the magnetosphere due to interaction with the solar wind [Lamy et al., 2017]. The aurorae emission is a reflection of the interaction between the solar wind and the magnetosphere. By investigating the cusp emissions, we can determine more details about how the charged particles of the solar wind inject into the atmosphere via the cusp region. Moreover, the tail reconnection can also trigger aurorae emissions by magnetospheric convection. Therefore, aurorae emission is very important for studying the magnetosphere of Uranus. Questions (3) and (4) about the magnetopause provided in Chapter 1 are directly related to the study of the aurorae emission because by studying the variation in the magnetopause's structure, which is formed by the interaction with the solar

wind, we can investigate the relationship between the cusp structure at the magnetopause and the disturbance of aurorae emissions.

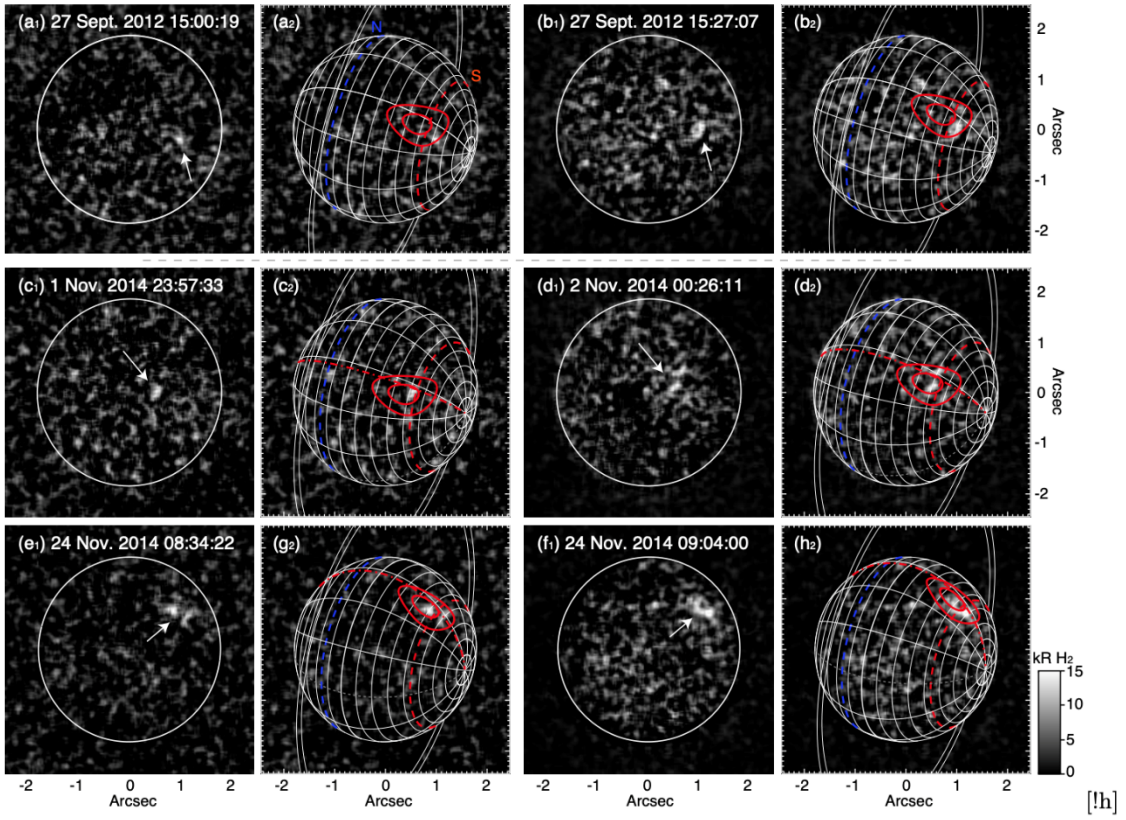

Figure 2.4 The images from Hubble Space Telescope for Uranus' past equinox. The images (a) and (b) were observed in 2012 and the other were in 2014. The red and blue dashed lines are respectively southern and northern magnetic poles. (Lamy et al., 2017)

Lam and Trafton studied the aurora on Uranus via H_3^+ emission from the ionosphere [Lam et al., 1997] [Trafton et al., 1999]. Melin et al. [2011] used infrared ground-based observations to study the seasonal variations in the ionosphere of Uranus and found that the solar ionization of atmospheric neutrons or seasonally changing current systems may play an important role in conductivity of the ionosphere.

2.3 Previous modeling studies

Because optical observations are limited to measuring local magnetospheric events, such as aurorae emissions, it is difficult to remotely study the global configuration of Uranus. Therefore, we need modeling simulations to validate the observational data and to enhance our understanding of the magnetosphere of Uranus. If a model fits observational data very well, it can provide further predictions for future spacecraft missions.

There have been some models that have studied the magnetosphere of Uranus in recent years. They addressed some specific scientific questions by using some assumptions in their models. However, these models also have limitations in their study of the magnetosphere due to these assumptions.

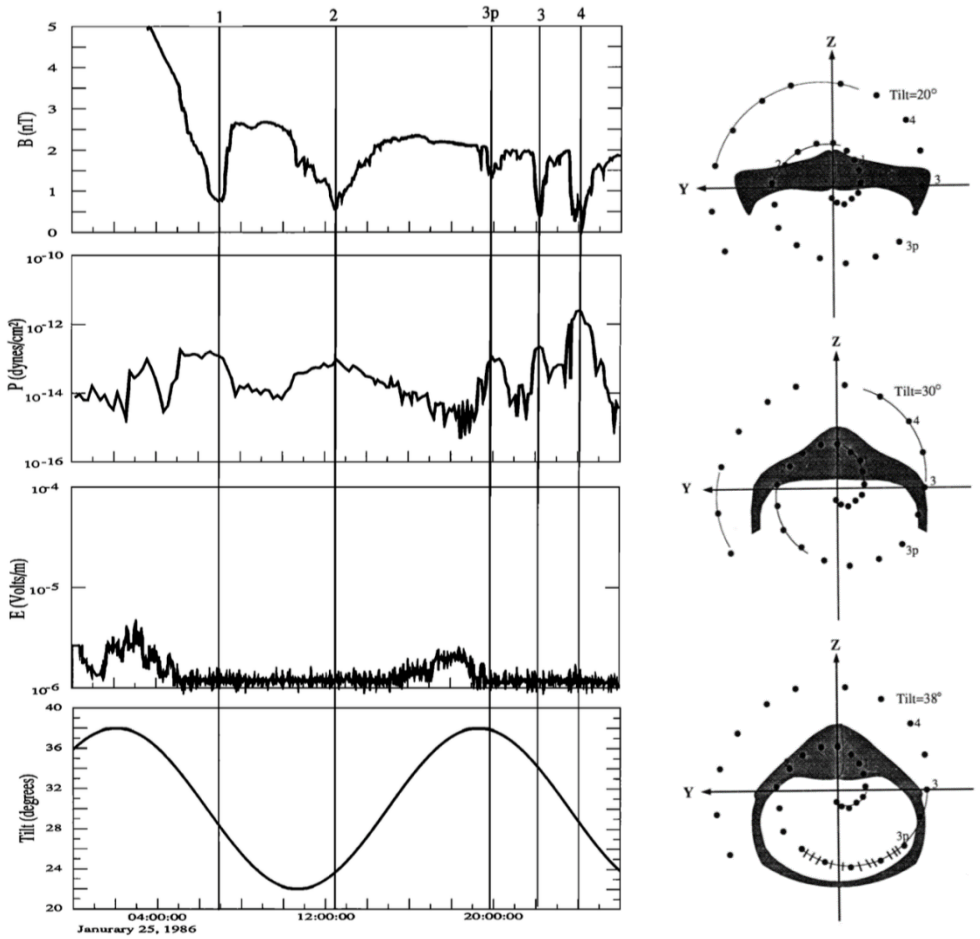

Figure 2.5 The left side reveals four different parameters (magnetic field strength, ion pressure, electric field and dipole tilt angle) measured by Voyager 2 with the spacecraft flying-by time. The vertical lines indicate the encounter event of the plasma sheet (Hammond et al., 1990). The right side reveals the simulation result which was described in (Hammond et al., 1990) and (Walker et al., 1989). The left side reveals the contours of the pressure, and the right side reveals the plasma sheet structure. The dipole tilt angle of both sides is respectively: 22°, 30° and 38°.

Hammond et al. [1990] and Walker et al. [1989] used a MHD model to simulate the curved sheet at the tail region by using a dipole tilt angle of 22°, 30° and 38°. The simulation described that the curvature of the current sheet varies with the dipole tilt angle, and they concluded that the dynamically curved current sheet was caused by the unique magnetic and rotational orientations as shown in Figure 2.5.

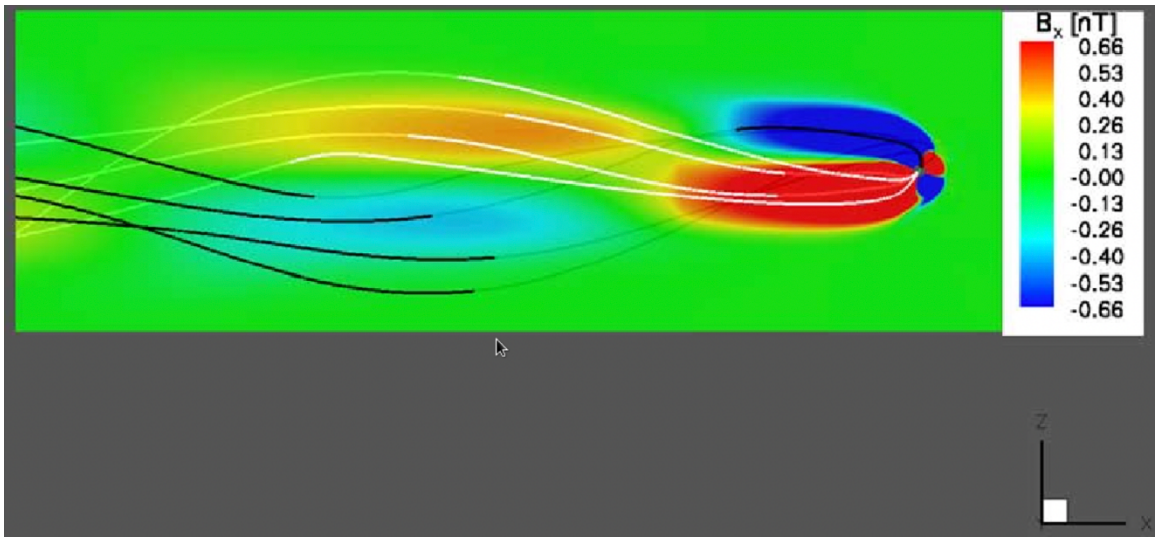

Figure 2.6 The twisted magnetotail structure in the XZ plane, which is produced by a single fluid MHD model (Tóth et al., 2004). The color difference means the different B_x component of the magnetic field.

Tóth et al. [2004] used a single fluid MHD model to simulate the magnetosphere of Uranus during the solstice season. They used a method of applying a rotational solar wind and a fixed planetary magnetic field in the model to replace a fixed solar wind and a rotational planetary magnetic field. Their model revealed a twisted magnetotail structure in the downstream region as shown in Figure 2.6. The bow shock and magnetopause locations simulated by their model corresponded to the measurements taken by the Voyager 2 spacecraft.

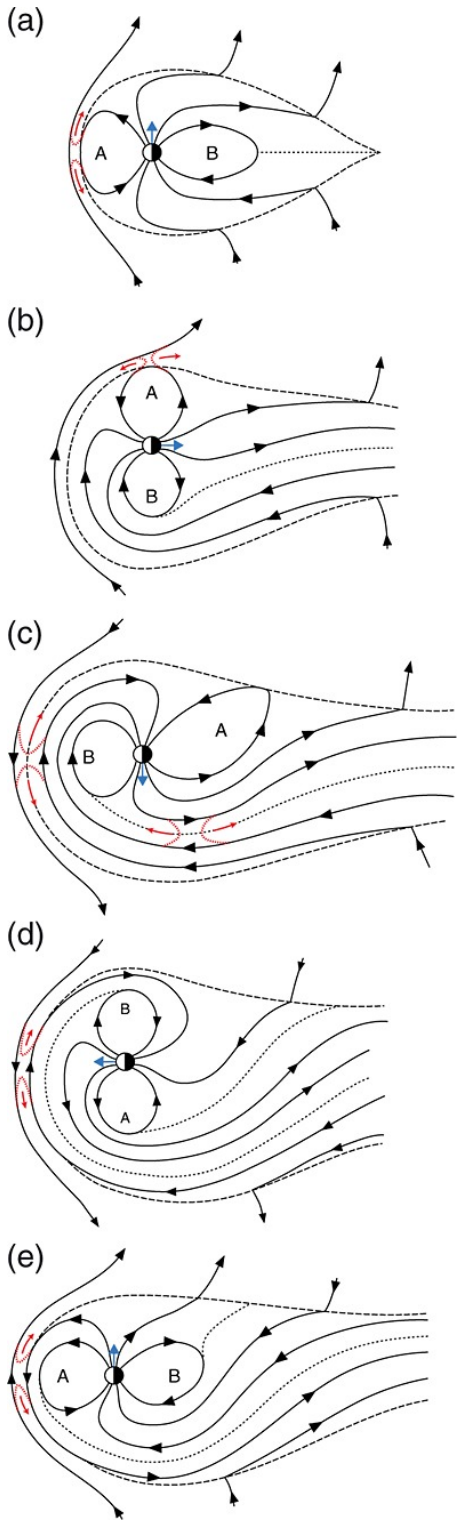

Figure 2.7 The evolution of the magnetic field lines of Uranus in the autumnal equinox season. The reconnection regions are indicated by the red arrows (Cowley, 2013).

Cowley [2013] analyzed the magnetosphere of Uranus during the autumnal equinox season. He argued that wound open flux tubes may be the reason why the weaker aurorae observations were caused by solar wind compressions for the near-equinox season as shown in Figure 2.7. However, how the tail reconnection occurs and how it affects the open flux tubes is still not clearly understood. Regardless, the difference in the magnetosphere of Uranus between the solstice and equinox is significant.

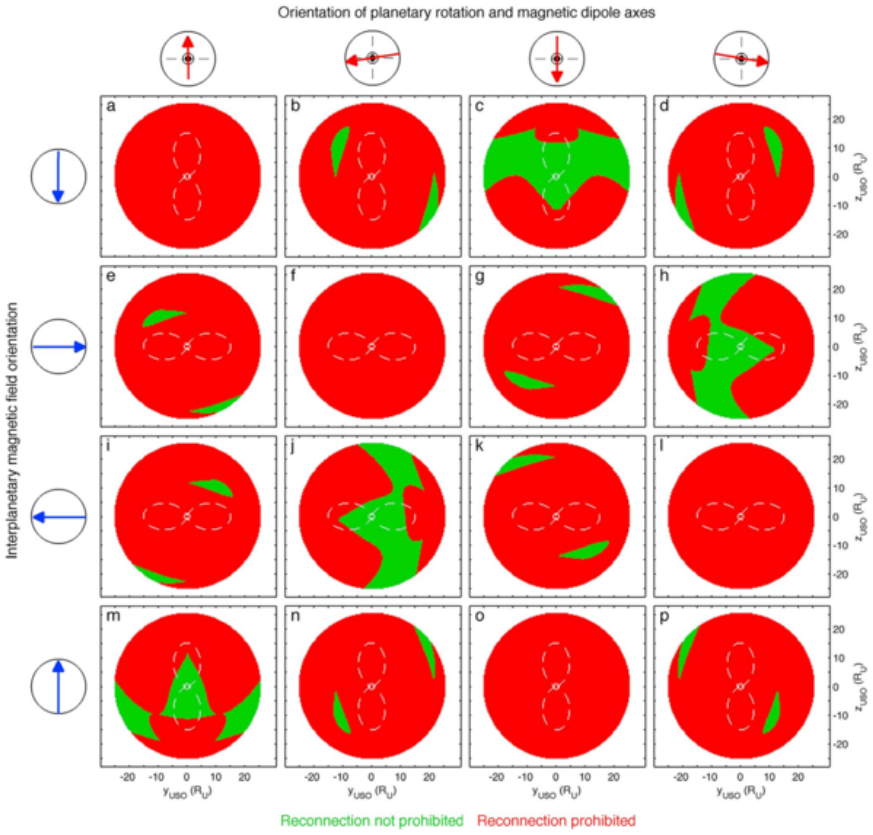

Figure 2.8 The regions at Uranus magnetopause where the reconnection is prohibited (red color) and not prohibited (green color) in Adam Masters' analytical model, during the northern winter solstice season. The red arrow shows the magnetic axis orientation and the blue arrow shows the IMF orientation (Masters, 2014).

To investigate the dayside interaction with the solar wind during the solstice and equinox, Masters [2014] used an analytical model to calculate the locations at the

magnetopause where the dayside reconnection is favorable or not favorable. Figure 2.8 shows the respective corresponding regions during the solstice season. Clearly, the reconnection region is highly dependent on the planetary rotation. Moreover, between different IMF orientations, favorable reconnection regions are not exactly symmetric with each other, which may be because the rotational axis does not exactly point toward the Sun.

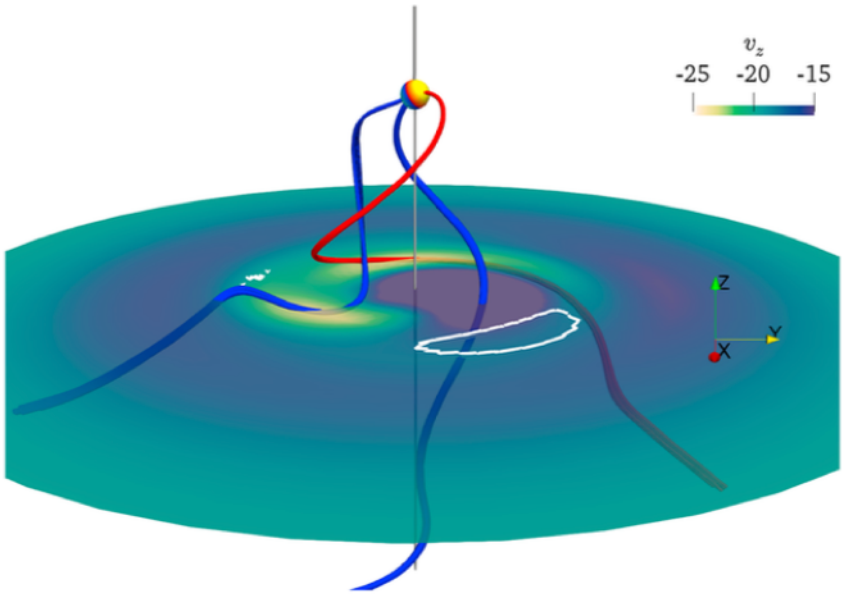

Figure 2.9 The magnetic field lines sourced from different magnetic poles of Uranus, extending to the tail direction (downstream). (Griton et al., 2017)

Griton et al. [2017] used a single fluid MHD model to investigate a Uranus-like magnetosphere. They artificially sped up the planetary rotational rate by 10 times that of Uranus to enhance the twisted effect of the magnetotail as shown in Figure 2.9. The results revealed that rapid rotation dominates the structure of the magnetotail of Uranus, which corresponds with the previous model by Tóth et al. [2004].

2.4 Limitations of previous modeling work

Although the progress in modeling studies of the magnetosphere of Uranus is significant, many of them have their limitations. For instance, Tóth et al. [2004] used a single fluid MHD model that is not able to separately track different ions and electronic species. Moreover, since their model used a method of fixing the simulation in coordinates that corotate with the planet, it may not be easy to apply the model to the equinox case. However, their model assumed a zero IMF for the upstream solar wind condition, which was deficient for studying the dayside reconnection at the magnetopause and the interaction with the solar wind. Masters [2014] studied the favorable reconnection locations at the magnetopause using an analytical model; however the model used a simplified magnetopause structure that was not the same as the MHD result. Griton et al. [2017] used a MHD model to focus on the twisted structure of a Uranus-like magnetosphere at solstice because they used a rotation rate that was ten times faster than the actual rate of Uranus. Moreover, their model did not include either the off-centered dipole or the unaligned rotational axis with the direction to the Sun. Mejnertsen et al. [2016] used a MHD model to study the magnetosphere of another ice giant, Neptune, specifically during the solstice season; however, their model is deficient concerning the offset dipole, which is 0.5 radii away from the planetary center. The offset dipole is very important for both the magnetospheres of Uranus and Neptune because it determines the dynamics in the near-space regions, such as the aurorae emissions or the injection of energetically charged particle through the cusp regions, which is essential for studying observational data. There were no numerical models that were able to simulate the global magnetosphere of Uranus and the diurnal variation of the dayside reconnection for both the solstice and equinox seasons until a recent study [Cao and Paty, 2017]. This model is able to simulate the

magnetosphere of Uranus, Neptune, exoplanets and any other planets that have any rotational and magnetic dipole geometry during any orbital seasons, including the solstice, equinox and seasons between the solstice and equinox.

Our multifluid MHD model contains all of the major characteristics of the rotational, magnetic and seasonal geometries of Uranus. First, the rotational axis is oriented in the exact direction as Voyager 2's measurements, which is 7.9° from the direction towards the Sun. Second, the magnetic orientation is 59° away from the rotational axis, which corresponds to Voyager 2's measurements as well. Third, the magnetic dipole moment in our model is offset by 1/3 R_U (Radii of Uranus) as is that of Uranus. Fourth, we used an actual average IMF from Voyager 2's magnetometer data, which enables us to investigate the influence of the dayside reconnection with the solar wind in a global magnetospheric configuration. Additionally, our model can use different IMF conditions to study the effect of the IMF. Finally, our model can investigate the magnetosphere of Uranus during different seasons, including the solstice, equinox and any other season between the solstice and equinox.

2.5 Rotational and magnetic structure and geometric transformation

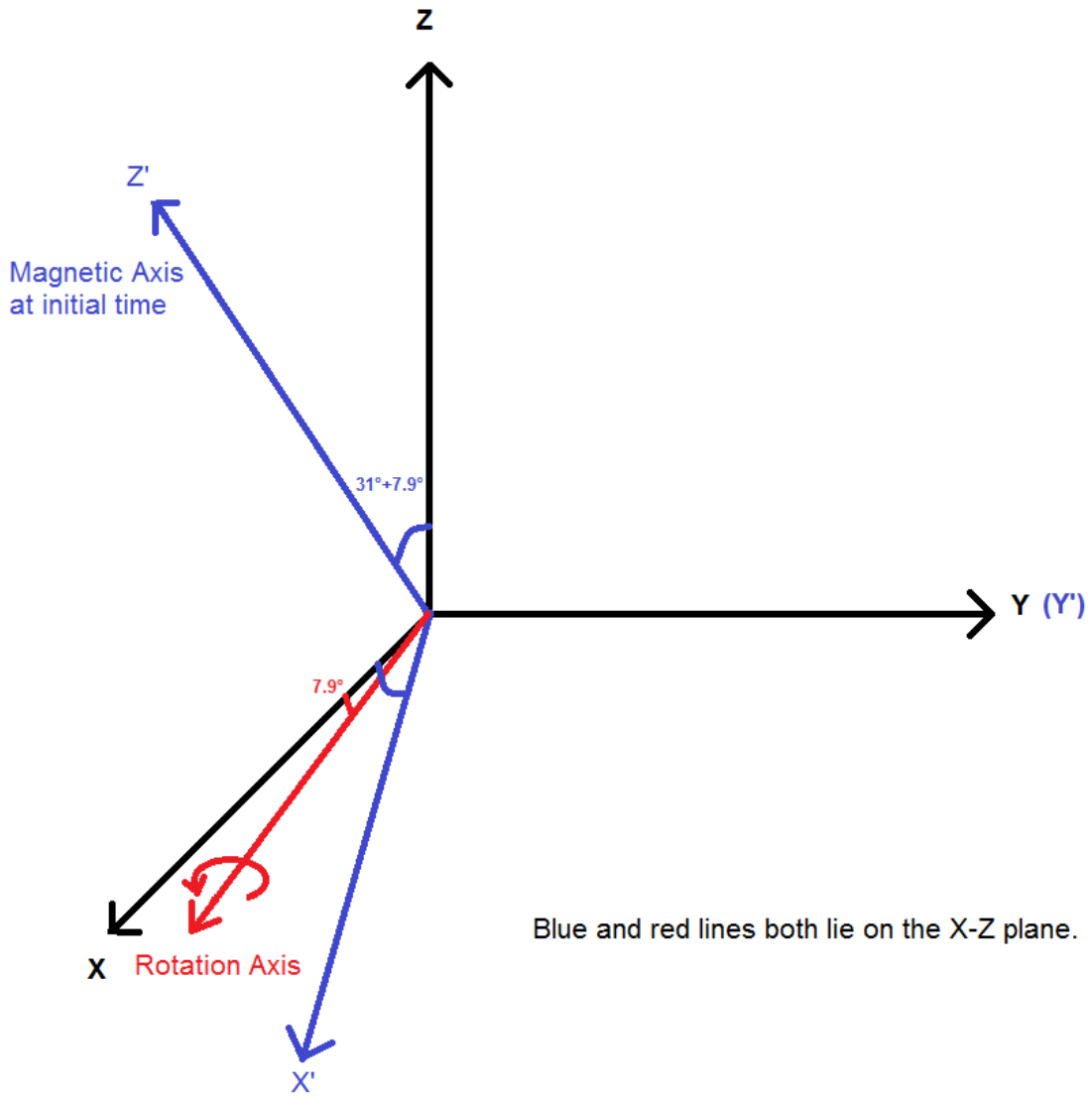

Figure 2.10 The rotational strategy of the planetary magnetic dipole field.

Our model uses a rotational strategy for the dynamic magnetic dipole field of Uranus. As shown in Figure 2.10, first, we defined a static coordinate system, XYZ, in which the X-axis points towards to the Sun, the Z-axis points towards the northern direction perpendicular to the solar wind direction and the Y-axis points perpendicular to both X and Z such that the X-, Y-, Z-axes obey the right-hand rule. This is slightly different from the original coordinates in our model, which will be discussed in the next chapter. However,

to make our strategy easier to understand and to better demonstrate it without further geometric transformation, we simply used the coordinates described above. Second, we rotated the coordinates counterclockwise around the Y-axis by 38.9° to obtain new coordinates of X'Y'Z', and the orientation of the Z' axis after this rotation points to the magnetic northern dipole's orientation, which was the initial setup for the dipole direction in our model. Third, we defined the rotational axis by rotating the X-axis counterclockwise around the original Y-axis by 7.9°. Then, the last step was to rotate the planetary magnetic dipole, which was initially set up for the X'Y'Z' coordinates around the rotational axis by a certain degree for the planetary rotation. Of note, the original points of the coordinates were shifted by 1/3 Ru (radii of Uranus) from the planetary center.

CHAPTER 3. DIURNAL AND SEASONAL VARIABILITY OF URANUS'S MAGNETOSPHERE

3.1 Summary

In order to study the coupling mechanism between the solar wind and the magnetosphere, we use a numerical model to simulate the global magnetosphere and to predict potential favorable reconnection locations. We investigated the existence of a "switch-like" magnetosphere at Uranus for both equinox and solstice seasons, where the planetary rotation drives the interchange between an open magnetosphere and a closed magnetosphere each Uranus day. This periodic reconnection is predicted to occur upstream of the magnetopause, with a frequency that corresponds to the planetary rotation (once per 17.24 h). The locations of the bow shock and magnetopause in our model are validated against measurements made by Voyager 2. In examining the evolution of the magnetic field configuration along with that of high plasma beta regions, which in combination indicate where the system is favorable for reconnection, we found that the reconnection that occurs is highly dependent on the rotation of the planetary magnetic field in both equinox and solstice seasons. These periodic reconnection events in our simulation support the hypothesis of a periodic "switch-like" magnetosphere at Uranus.

3.2 Introduction

The study of Uranus's magnetosphere has been limited in the decades since the Voyager 2 spacecraft flew by Uranus in 1986. Due to its high obliquity, off-centered, and highly tilted dipole, Uranus's magnetosphere provides an important virtual laboratory for

studying seasonality of magnetospheric dynamics. At an average location of 19 AU, the dynamic pressure of the solar wind at Uranus is considerably weaker than at Earth. Uranus's complex magnetic and rotational geometry generates a dynamic magnetosphere that has fascinated scientists for decades. In this paper we focus on understanding the structure and dynamics of Uranus's magnetosphere. The only in situ observations of Uranus were made by the Voyager 2 spacecraft in 1986. The measurements made by the Triaxial Fluxgate Magnetometer (MAG) revealed that the magnetic field of Uranus is quite distinct from those of the terrestrial and gas giant planets. The obliquity of Uranus's rotation axis is 97.9°, and there is a 59° angle between the rotation axis and the magnetic axis. Also, the magnetic dipole moment is off-centered by 1/3 Ru (radii of Uranus) toward the south pole. Uranus's rotation axis is approximately parallel to the ecliptic plane and was pointing almost directly to the Sun during solstice season when the 1986 flyby took place. In this paper, we will focus our modeling efforts on understanding the dynamics, structure, and seasonal variability of the magnetosphere of Uranus. The study of the magnetospheres of ice giants is broadly relevant because they are natural templates for the magnetospheres of many analogous exoplanets, and our model could be applied to further understanding these recently discovered worlds.

From the measurements taken by the Voyager 2 spacecraft, we have learned that Uranus's magnetosphere is different from those that we have previously observed from the terrestrial and gas giant planets. For example, solar wind-driven magnetospheric convection is dominant in Uranus's magnetosphere, although the rotation-driven dynamics are not negligible [Vasyliunas, 1986; Ye and Hill, 1994]. It is not surprising that the influence of corotation on the magnetospheric plasma is important because Uranus is a

relatively fast rotator with a period of 17.24 h. However, the frequent magnetic reconnection events at the magnetopause, due to the parallel and antiparallel alternation between the interplanetary magnetic field (IMF) and planetary magnetic field, can dominate the input of momentum and energy from the solar wind into the magnetosphere. Essentially, this produces a "switch-like" magnetosphere alternating between open and closed configurations. Voigt et al. [1987] predicted that the magnetosphere at solstice would vary periodically from an open to a closed structure and back using theoretical model calculations. Although there has not been an observational study about the dynamic variations at Uranus, the potential importance of magnetic reconnection on global magnetospheric dynamics has been explored for the case of Earth's magnetosphere at northern and southern oriented IMF [Korth et al., 2005; Li et al., 2011; Liu et al., 2012; Lu et al., 2013]. Mejnertsen et al. [2016] reported similar global magnetospheric variation in the case of Neptune, another ice giant with a highly tilted dipole axis.

The aurora provides an expression of dynamics inside the magnetosphere, which can be used to trace the plasma convection, magnetic reconnection, and injection of energetic charged particles into a planet's atmosphere. Due to the magnetic field topology produced by the shifted dipole, the auroral regions should appear much closer to the geometric equator rather than the poles [Connerney, 1993]. Observations of the UV aurora of Uranus made by Hubble Space Telescope (HST) in recent years confirmed this assumed latitudinal distribution of auroras [Lamy et al., 2012].

By examining the aurora at Uranus, researchers gained insight into the composition, temperature, and density of plasma in the ionosphere as well. The aurora emission spectrum depends on the composition of the ionosphere, and previous studies revealed that the

ionosphere of Uranus consists of charged particle species including electrons, protons, trihydrogen cation (H3+), and other heavy ions, providing a source of plasma to the magnetosphere [Atreya and Donahue, 1975; Chandler and Waite, 1986; Majeed et al., 2004]. The electron density of the ionosphere can reach 105–106 amu/cm3 [Chandler and Waite, 1986; Waite and Cravens, 1987; Lindal et al., 1987; Majeed et al., 2004].

Behannon et al. [1987] demonstrated from Voyager 2 observations that Uranus's magnetotail lobes have an average pitch angle of the helical twist of about 5.5° and that the plasma sheet is parabolically curved with a nonuniform thickness. There have been several empirical models that describe the asymmetries found in a tilted magnetosphere. For example, Schulz and McNab [1996] simulated that different tilt angles of a magnetic axis could result in different structures in the plasma sheet. Voigt et al. [1987] demonstrated that the curvature of Uranus's plasma sheet varied with the planetary rotation. However, there were several questions that remained unanswered. For instance, what is the thickness of the tail plasma sheet, and does the dawn- dusk asymmetry in the plasma sheet vary in time?

Another important question is how the global magnetosphere is structured far from the planetary surface. Masters [2014] used an analytical model to study the periodic variation of magnetic reconnection at Uranus. He found that geometries favoring reconnection were highly related to the planetary rotation. Tóth et al. [2004] developed a time-dependent numerical model of Uranus magnetosphere in order to investigate the twisted magnetotail during solstice. This MHD (magnetohydrodynamic) simulation assumed that the IMF could be ignored, it was equal to zero. However, the magnetospheric structure during equinox was not numerically modeled and there have been no plasma

dynamic modeling studies investigating reconnection in Uranus's magnetosphere through its interaction with the solar wind IMF. This is likely due to the difficulty in modeling Uranus's complex, rotating magnetic structure, while also including the incident IMF orientation. The seasonal variation of the magnetospheric structure also requires much adaptability in the boundary conditions of the simulation. Here we present results from our newly developed, and generalized, simulation of Uranus's magnetosphere interacting with the IMF during both solstice and equinox conditions. Our study reveals that although solar wind-driven magnetospheric convection is dominant in the global system, high magnetic latitude reconnection near the polar region also plays an important role in the plasma processes and magnetic structure inside of the magnetosphere. The periodic reconnection on the dayside magnetopause in the simulation supports the hypothesis of a "switch-like" magnetosphere. Our model indicates a dynamic asymmetry of the plasma sheet in the magnetotail for the first time and predicts the approximate thickness of the tail plasma sheet. The results also reveal the dynamically varying curvature of the tail plasma sheet during one Uranus day, which is consistent with the theoretical model calculations [Voigt et al., 1987].

3.3 Methodology

3.3.1 Multifluid MHD Model

Our model is based on the multifluid MHD model of Winglee [1998], which is a plasma dynamic model designed to study the interaction of the interplanetary solar wind with the intrinsic magnetic field of a planet. This modeling approach provides the context necessary to interpret the spatially and temporally sparse observations for Uranus. This

model has already simulated several planetary magnetospheric configurations as well as ionospheric interactions of planetary magnetospheres with icy moons. Examples include studies of the Earth's magnetosphere [Winglee, 1998], Ganymede's magnetosphere[Paty and Winglee, 2004; Paty and Winglee, 2006] and the Saturn-Titan coupled magnetospheric system [Winglee et al., 2009]. Our model considers separate fluids for electrons and different ion species, as is shown in equations (1)-(6). Bagenal et al. [1987] pointed out that the single-fluid description of this system would not accurately describe the ion and electron plasma pressure contributions to the overall structure of Uranus' magnetosphere. Our multifluid model explicitly tracks the pressures of each ion fluid as well as that of the electrons. This is important, because (I) the ionosphere consists of multiple ions [Atreya et al., 1975; Chandler et al., 1986; Majeed et al., 2004], which could affect to some extent the magnetospheric dynamics and auroral emissions. Therefore, tracking individual plasma species is necessary. (II) Our model can track ion and electron species separately from different sources. For instance, while solar-wind-driven magnetospheric convection dominates the system, the ionospheric plasma outflow is also important, especially for the inner magnetosphere. Using our model, we can track protons sourced exclusively from the solar wind and study how the frequent dayside reconnection at the magnetopause drives plasma convection inside the magnetosphere. We can also separately track the different polar wind species from the ionosphere in order to study their effect on the magnetosphere.

The basic equations of the multifluid MHD model are shown below. Equations (1) and (2) are the conservation equations of mass and momentum for each plasma species respectively, and equation (3) is equation of state for each ion species and the electrons. Equations (4) and (5) are the relationship of density and velocity of ions and electrons, and

the evolution of the magnetic field (based on Maxwell's equations). Equation (6) is the generalized Ohm's law [Winglee, et al., 2009]. In the equations above, ρ represents the mass density of a fluid, **V** is the fluid velocity, P is the pressure for positive ions and electrons in equation (3), **E** and **B** are electric and magnetic field respectively, **J** is the electric current density, n_i and n_e are the number density of ions and electrons respectively, and γ is the ratio of specific heats. Unlike traditional MHD, the equations can describe different ions as individual fluids. In order to satisfy the conservation of charge that is the requirement of quasi-neutrality, the sum of total positive charges equals to the sum of total negative charges (e.g. Eq. 4), if we assume that the ions are all singly charged particles. In our simulation, the conductivity, σ, is finite in the ionosphere compared to anywhere else in the magnetosphere, which is treated as perfectly conducting. The conductivity can be described as a tensor containing the Pedersen conductivity, Hall conductively, and parallel conductivity. However, since we assume the collision frequency with neutrals in the ionosphere is relatively high, the Pedersen conductivity is equal to the parallel conductivity, and the Hall conductivity goes to zero so that the conductivity in our model is isotropic and a scalar. In equation (6) this is represented by the resistivity (η), where $\sigma = (\frac{1}{\eta})$.

$$\frac{\partial \rho_\alpha}{\partial t} + \nabla \cdot (\rho_\alpha \boldsymbol{V}_\alpha) = 0 \qquad (1)$$

$$\rho_\alpha \frac{\partial \boldsymbol{V}_\alpha}{\partial t} = q_\alpha n_\alpha (\boldsymbol{E} + \boldsymbol{V}_\alpha \times \boldsymbol{B}) - \nabla P_\alpha - \left(\frac{GM}{R^2}\right) \rho_\alpha \hat{\mathbf{r}} \qquad (2)$$

$$\frac{\partial P_\alpha}{\partial t} = -\gamma \nabla \cdot (P_\alpha \boldsymbol{V}_\alpha) + (\gamma - 1) \boldsymbol{V}_\alpha \cdot \nabla P_\alpha \qquad (3)$$

$$n_e = \sum_i n_i \ , \quad \boldsymbol{V}_e = \sum_i \frac{n_i}{n_e} \boldsymbol{V}_i - \frac{\boldsymbol{J}}{e n_e} \ , \quad \boldsymbol{J} = \frac{1}{\mu_0} \nabla \times \boldsymbol{B} \qquad (4)$$

$$\frac{\partial \boldsymbol{B}_p}{\partial t} + \nabla \times \boldsymbol{E} = \boldsymbol{0} \qquad (5)$$

$$\boldsymbol{E} = - \sum_i \frac{n_i}{n_e} \boldsymbol{V}_i \times \boldsymbol{B} + \frac{\boldsymbol{J} \times \boldsymbol{B}}{e n_e} - \frac{1}{e n_e} \nabla P_e + \eta(x) \boldsymbol{J} \qquad (6)$$

3.3.2 Nested grid system and rotational field

We apply the multifluid MHD equations to a nested grid system with appropriate inner and outer boundaries discussed below. This model is built on a three dimensional Cartesian coordinate system which enables us to divide three dimensional space into a number of cells whose sizes in different boxes measure their local space resolution. The center of the planet is located at the origin of the coordinates in the innermost box whose resolution is highest in the model. In our model for Uranus, we used five boxes with different spatial resolutions in the USO (Uranus Solar Orbital) coordinate system, which is defined by the X axis pointing away from the Sun, the Y axis lying in the orbital plane and parallel to the orbital velocity of Uranus, and the Z axis completes the right-handed system. The simulation region extends from -100 R_u upstream to +124 R_u downstream in the X direction, and from -128 R_u to 128 R_u in the Y and Z directions. The finest resolution in our model is 0.2 R_u in the inner box and the coarsest resolution, in the outermost box, is 3.2 R_u, with each nested box decreasing in resolution by a factor of 2. Based on the average IMF strength measured by Voyager 2, which will be discussed in the following section, we set the IMF in the model oriented in the -Z dirention with 0.1 nT strength.

For our model, we adopted the method of a three dimensional time dependent space rotational transformation in order to rotate the magnetic dipole which is fixed to the rotation of the planet. We applied the geometric rotation to the dipole's rotation in the model. This geometric rotation is widely applied in a variety of science and engineering areas, such as particle physics [Battey-Pratt et al., 1980]. This differs from the approach in Tóth et al., (2004), where there is a rotation of the solar wind but a fixed dipole. The basic logic of our modification is using a time varying offset tilted dipole field $\mathbf{B}_{0,rot}(x, y, z, t)$ to represent the planetary intrinsic field. The total magnetic field **B** used in the equation (2, 4, 6) is the sum of $\mathbf{B}_{0,rot}$ and the perturbation field $\mathbf{B}_p$, derived in equation (5). The offset tilted dipole (OTD) moment is located at the point (0.3302, 0.00, 0.0458) R_u with the orientation being tilted by 38.9° from the positive Z-axis towards the Sun initially for the solstice case, and at the point (0.00, -0.3302, 0.0458) R_u with the orientation being tilted by 38.9° from the positive Z-axis towards the positive Y direction initially for the equinox case. The dipole starts to rotate about the planetary rotation axis when $t > 0$. The period of rotation is 17.24 hours. Thus, the orientation of the dipole moment evolves back to its initial phase every 17.24 hours. This method of rotating the offset tilted dipole field enables us to track the plasma parameters instantaneously in the USO coordinate system without any transformation between non-inertial and inertial coordinate systems in each time step. This simplifies the calculation of our multifluid MHD equations in the inertial coordinate system.

3.3.3 Boundary conditions

We set the inner boundary at 3 R_u from the center of Uranus, and the ionospheric temperature in our model is 500 K. The ionosphere contains three charged particles species:

proton, trihydrogen cation (H_3^+) and electron. In order to tractably model the magnetosphere, we use an enhanced ionospheric density of 10,000 cm^{-3}. This reduces the Alfvén speed at the inner boundary. However, to avoid unrealistic outflows from the ionosphere, we also surpress its radial velocity. We set the ionospheric resistivity (η) in the model to 10^6 Ω·m, and the resistivity outside of the ionosphere is set to zero.

The solar wind condition is important because it dominates the interaction of the solar wind with the planetary magnetic field and thus drives magnetospheric convection [Vasyliunas, 1986]. Compared to the magnetospheres of Jupiter and Saturn, there exists no strong internal plasma source. The only data of the solar wind condition is obtained by Voyager 2 measurement in 1986. We use a solar wind density 0.1 amu/cm^3 in our model based on previous data-model validation [Tóth et al., 2004]. The interplanetary magnetic field (IMF) strength is relatively low compared with that near Earth due to Uranus' 19 AU distance from the Sun. However, the orientation and magnitude of the IMF plays an important role in dictating reconnection with the planetary field on the dayside magnetopause, and is non-negligible for studying the effect of periodic reconnection on magnetopheric convection. Xue et al. [1996] and Lepping et al. [1989] determined the average IMF strength measured by Voyager 2's magnetometer at Uranus to be ~0.1 nT with experimental uncertainties of 0.006 nT for each magnetic field component. We also analyzed data from Voyager 2's magnetometer, 3 hours prior to its crossing of Uranus' bowshock. In Figure 3.1, we plot the upstream magnetic field for this time period for all 3 components and the total field. The MAG data during this period shows B_x and B_y fluctuated above and below zero, but B_z fluctuated above and below about -0.08 nT, the fluctuation of total B is around 0.1 nT, which means the average magnetic field is mainly

contributed by B_z. Therefore, we let B_x and B_y equal zero, and oriented the total average |**B**| to the B_z direction, setting B_z to -0.1 nT. The upstream boundary of our model is 100 R_u upstream of Uranus, where Voyager 2 data was measured for the interplanetary solar wind. We assume a static IMF condition during our simulation in order to explore the changes to the magnetospheric morphology as Uranus' OTD field rotates. While the upstream data illustrates a dynamic and variable IMF, the complexity this adds to Uranus' magnetospheric dynamics is beyond the scope of this work.

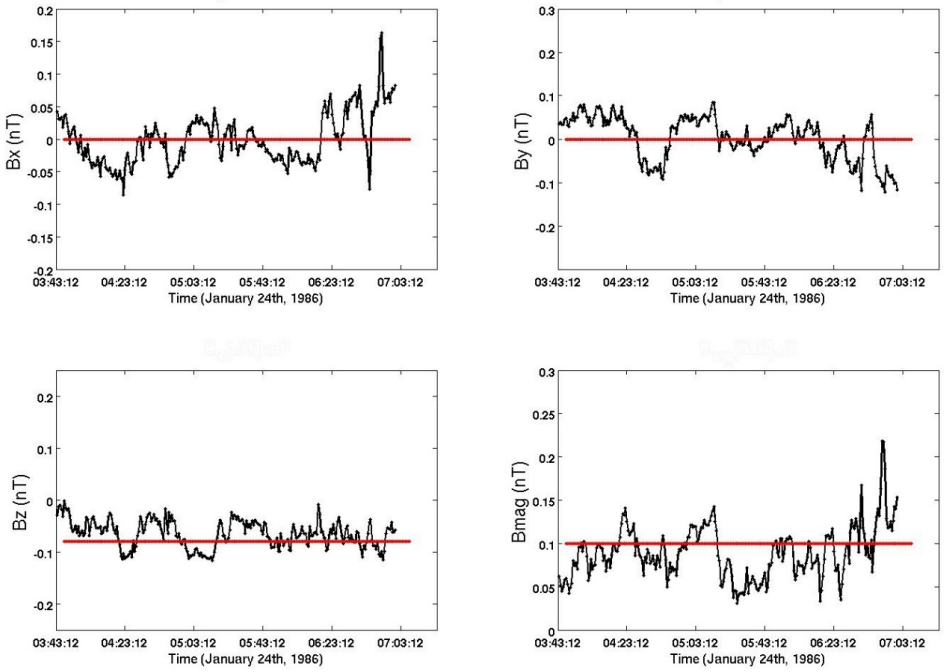

Figure 3.1 The IMF variations observed by Voyager 2 measurement on January 24th, 1986, about 3 hours before the spacecraft encountered the bow shock. The four panels shows B_x, B_y, B_z, and total magnitude of B. The black curves are the MAG data, and the red horizontal lines are the average of the fluctuating IMF during that time period.

3.4 Results and Discussion

As discussed in the methods section, the magnetic field in our simulation is divided into two parts: the unperturbed rotating dipole field $\mathbf{B_{0,rot}}$ and the perturbation field $\mathbf{B}_p$. $\mathbf{B}=\mathbf{B_{0,rot}}+\mathbf{B}_p$. Studies based on Voyager 2's measurements calculated that the bow shock location was about 23.4 R_u [Bridge et al., 1986; Gurnett et al., 1986 ; Ness et al., 1986, Xue et al, 1996]. This bow shock location is accurately reproduced by the simulation. The unperturbed magnetic field -- a rotating, tilted, and off-centered dipole field fixed with the rotating planet -- is consistent with the inner magnetosphere as observed by the Voyager 2 magnetometer. The bulk of our modeling work will now focus on diurnal and seasonal variations with respect to the dayside reconnection and the magnetospheric configuration.

For most planetary magnetospheres, reconnection at the dayside magnetopause plays a significant role in the penetration of solar wind into the magnetosphere. The situation at Uranus is more complicated as the OTD and high obliquity of the planetary magnetic field is rapidly changing in orientation with respect to the IMF. Also, reconnection occurs periodically when the two fields approach an anti-parallel configuration. The reconnection favorable area at the dayside magnetopause can reach as high as 15%-35% when the planetary magnetic moment approaches parallel to the IMF, but decreases to below 5% when the planetary magnetic moment approaches antiparallel in its rotation phase [Masters, 2014]. Voigt et al. [1987] analyzed that the IMF directly affects the magnetospheric convection process, which is periodically interrupted by the rotation of the planet. Based on these findings, we investigated that the solar wind plasma input into Uranus' magnetosphere should be modulated by the variation of the planet's rotation phase at seasons such as both equinox and solstice, most likely by the reconnection

variation at the magnetopause (i.e. a "switch-like" magnetosphere); a hypothesis we will explore in this section with our simulation results.

3.4.1 Equinox Case

How the magnetosphere of Uranus reorganizes itself at equinox is not clear [Arridge, 2015]. As discussed in Masters [2014], the plasma beta distribution on the global scale suggests reconnection-favorable regions where the frozen-in condition breaks down and enables magnetic diffusion and reconnection to occur. The plasma beta, which is the ratio of plasma pressure to magnetic pressure, is a local indicator that identifies if a region is dominated by plasma or by magnetic field. The frozen-in condition, where plasma moves with (and is tied to) the magnetic field, is the prevalent condition in the magnetic field dominated region where the plasma beta is less than 1. In these regions, the ideal MHD approximation is applicable. The diffusion regions form in plasma dominated locations where the plasma beta is larger than 1; this creates a local break-down in the frozen-in condition and provides conditions favorable for magnetic reconnection. In Figure 3.2 and Figure 3.3, we show the variation of total plasma pressure (left) and plasma beta (right) in the XZ plane during one full planetary rotation period, with magnetic field lines superimposed in the same plane for equinox conditions. This helps to illustrate where reconnection-favorable plasma beta is spatially correlated to reconnection-favorable magnetic alignment. The subpanels on the right side of the figure generally show that the high plasma beta regions fall along the magnetopause, which corresponds well with potential reconnection regions. The plasma beta inside the magnetosphere is much lower globally, except for near the current sheet. The prevalence of low plasma beta inside its magnetosphere reflects the lack of a significant interior plasma source. Each row of these

figures represents one of eight rotation phases, whose rotation angles are 0, 45, 90, 135, 180, 225, 270, 315 degrees (labeled (a) through (h), respectively).

The plasma beta in row (a) shows that the favorable reconnection regions are not located at the sub-solar point, but down stream along both flanks of the magnetopause. Combined with the magnetic field orientation, this produces local, high latitude reconnection, however, the overall structure of the magnetic field is that of a closed magnetospheric configuration [Lu et al., 2013]. Row (b) shows that the post-polar reconnection region in the southern hemisphere moves toward the dayside, and that in the northern hemisphere it moves toward the night side. This migration of the reconnection regions transitions the magnetosphere to an open magnetospheric configuration, where reconnection is located in the sub-solar and magnetotail regions. Row (c) shows a pole-on configuration where reconnection occurs on the southern dayside magnetopause. The southern hemisphere lobe is reduced in extent and closed, while a semi-open magnetic configuration appears in the northern hemisphere. This is the critical phase for the transition from a closed magnetosphere to an open magnetosphere during Uranus' rotation. Row (d) shows that an open magnetosphere forms with high latitude fields open to the IMF in both hemispheres. The sub-solar region reconnection and tail reconnection form with this phase having been reached, however the global structure is still quite asymmetric since the southern hemisphere switching to an open structure lags behind the northern hemisphere. In our paper, the terminology "switch on" and "switch off" respectively represent the process that the magnetosphere changes from closed to open structure and from open to closed structure.

When the rotation reaches 180 degrees from the initial phase (Figure 3.3), the open configuration of the magnetosphere reaches its maximum, with a large fraction of open magnetic field demonstrated in row (e). At this phase the sub-solar region reconnection is at its most favorable geometry, with the highly open polar magnetic field and the corresponding response of magnetic field structure in the magnetotail closely resembling a 'typical' convection magnetosphere. This global configuration exists only for this brief period of time in Uranus' rotation, with the magnetic alignment changing dramatically within a few hours. This is solid evidence that the planetary rotation affects the magnetosphere and that it differs from the case of a static (non-rotational) magnetosphere. Row (f) shows that the open structure dominates in the southern hemisphere, and is shrinking in the northern hemisphere as the rotation drives the field back to a closed configuration, what we call "switch-off". The dayside reconnection moves to higher latitude along the northern hemisphere magnetopause. In row (g) we again reach a pole-on configuration, oppositely oriented to that in row (c), with the magnetic north pole pointing toward the Sun in this plane. This is a critical transition from the open to closed structure, where the dayside field lines appear closed and sub-solar reconnection is less favorable. Finally, in row (h) the polar reconnection region migrates toward the night side and downstream of Uranus, and the magnetospheric structure appears completely closed (or "switched-off") to the solar wind.

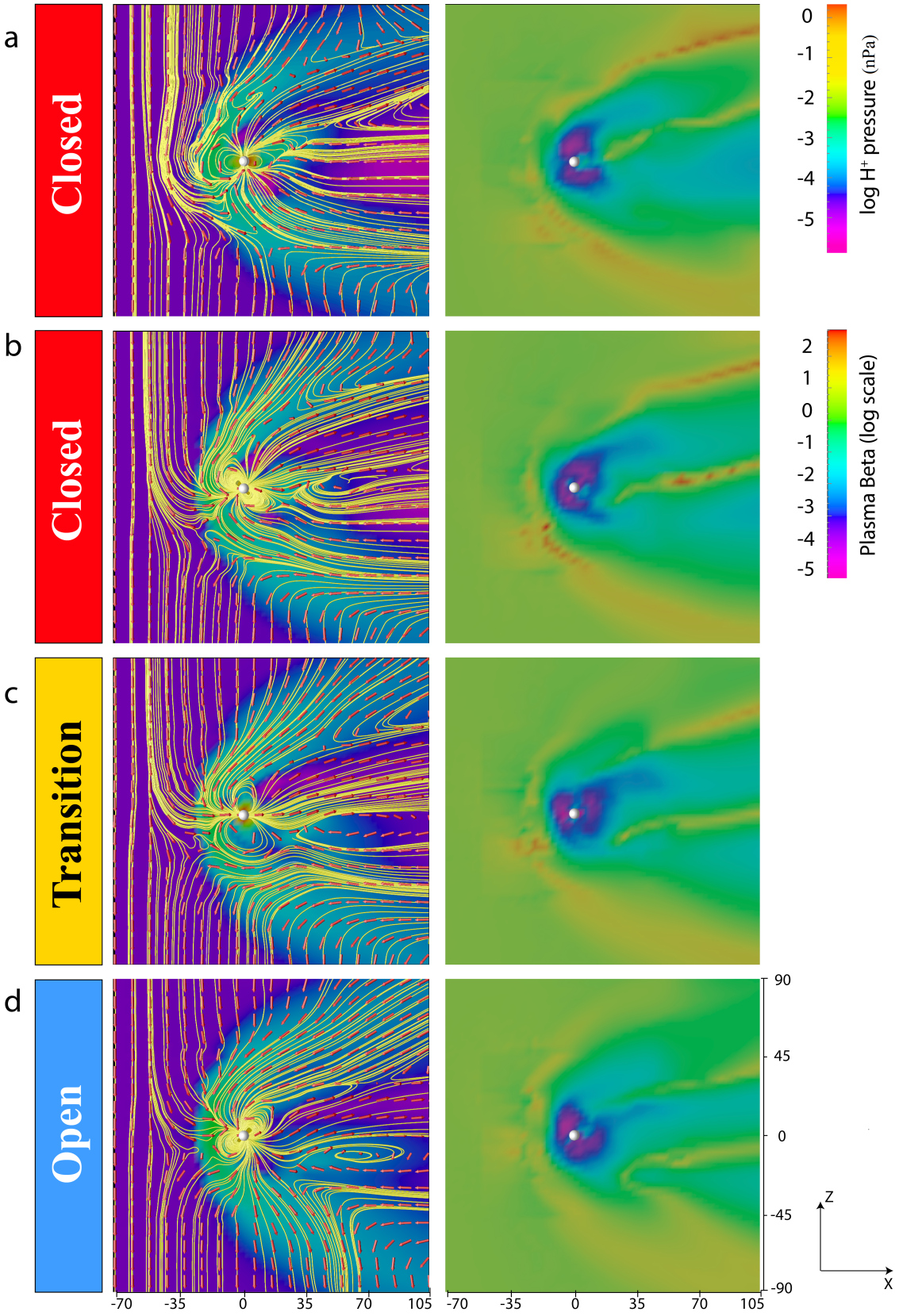
a
Closed
b
Closed
c
Transition
d
Open
0
-1
-2
-3
-4
-5
log H+ pressure (nPa)
2
1
0
-1
-2
-3
-4
-5
Plasma Beta (log scale)
-70
-35
0
35
70
105
90
45
0
-45
-90
Z
X

Figure 3.2 The logarithm of the H+ pressure and of the plasma beta in the XZ plane at equinox are shown in the left and right column, respectively. Both color bars are displayed at the top right corner. The magnetic field lines are represented in yellow in the left column, and the red arrows represent the direction of the magnetic field. The labels at the far left indicate if the global configuration of the magnetosphere is closed, open or transition between closed and open. This figure displays the first half of the planetary rotation period.

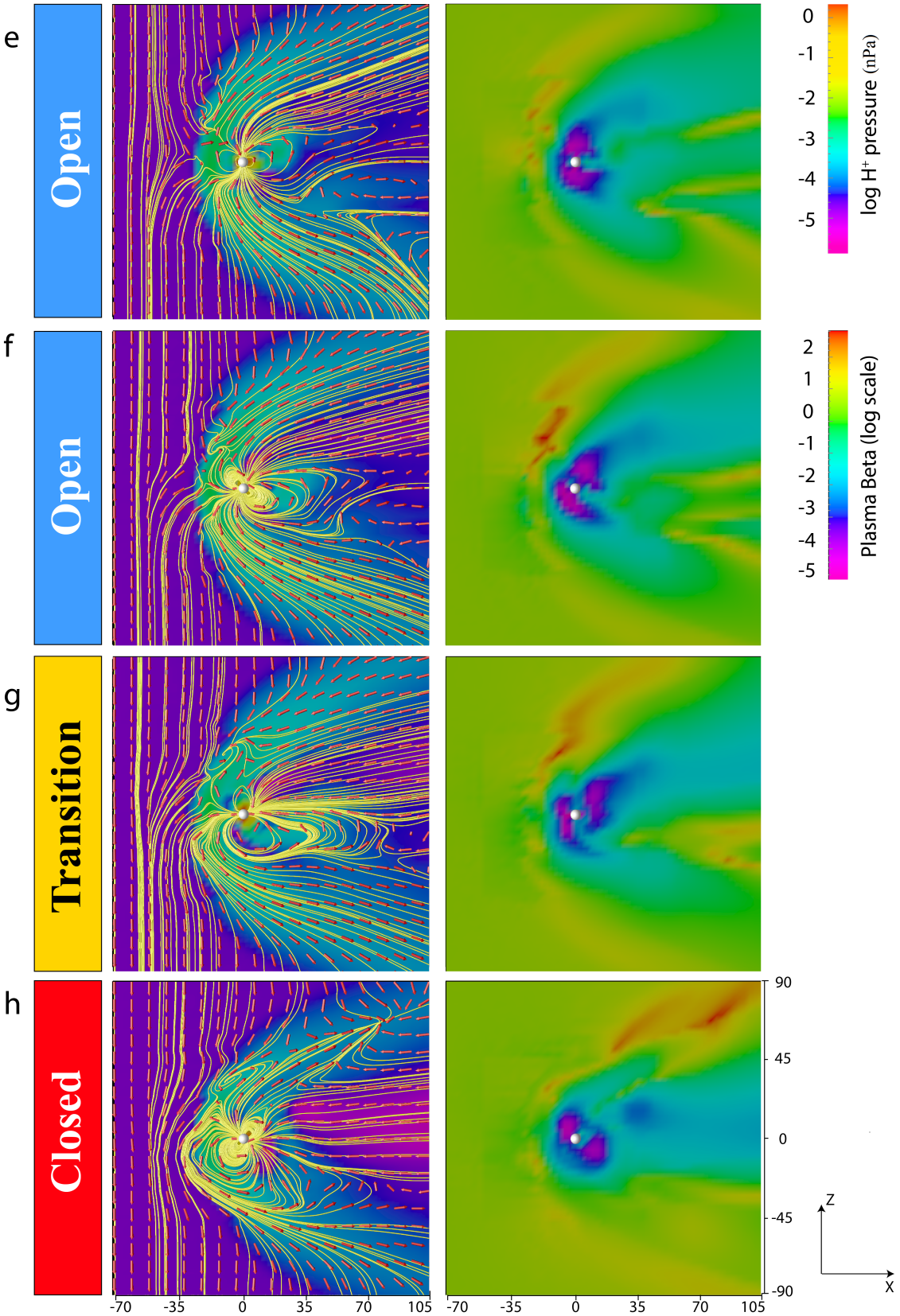
e
Open
f
Open
g
Transition
h
Closed
0
-1
-2
-3
-4
-5
log H+ pressure (nPa)
2
1
0
-1
-2
-3
-4
-5
Plasma Beta (log scale)
-70
-35
0
35
70
105
90
45
0
-45
-90
Z
X

Figure 3.3 The logarithm of the H^+ pressure and of the plasma beta in the XZ plane at equinox are shown in the left and right column, respectively. Both color bars are displayed at the top right corner. The magnetic field lines are represented in yellow in the left column, and the red arrows represent the direction of the magnetic field. The labels at the far left indicate if the global configuration of the magnetosphere is closed, open or transition between closed and open. This figure displays the second half of the planetary rotation period.

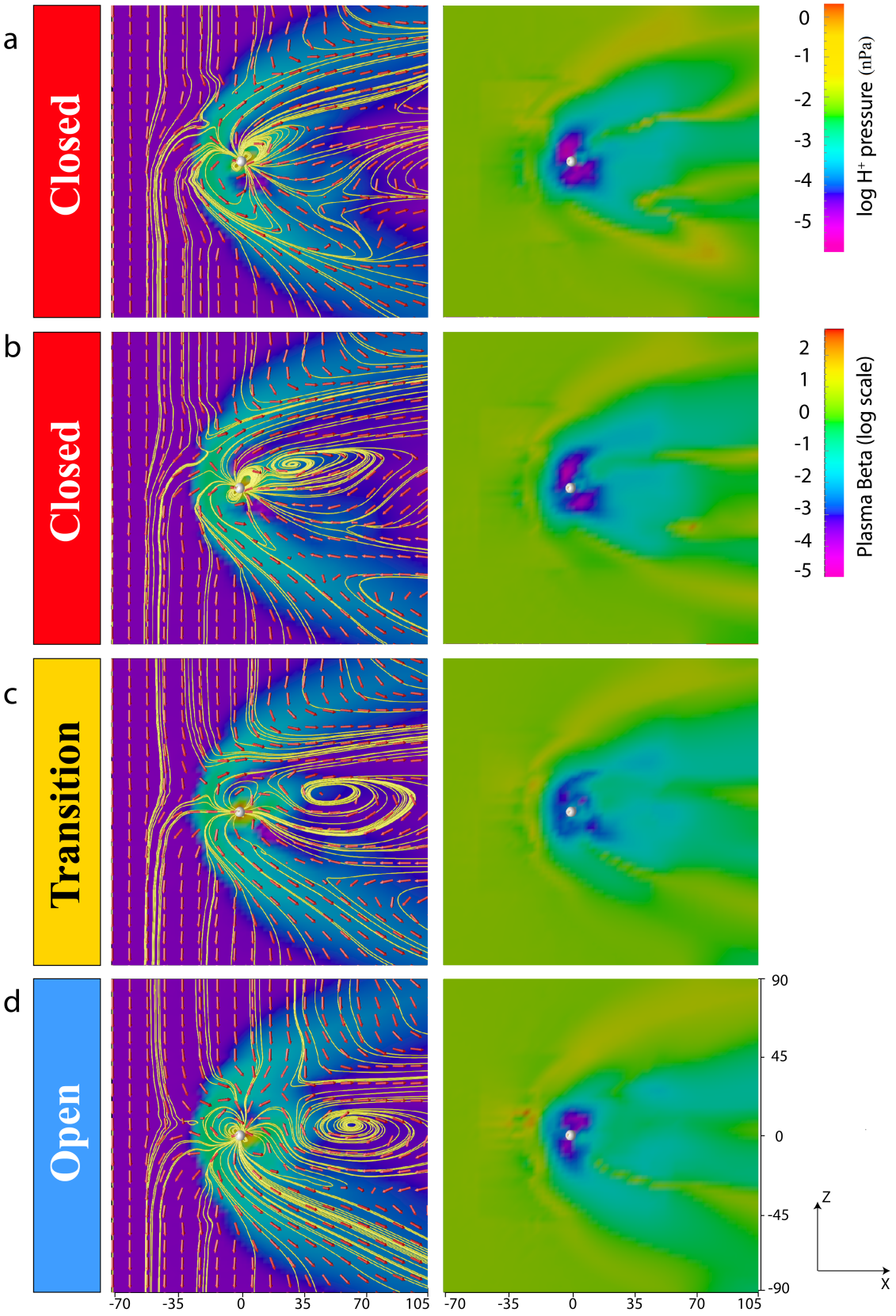
a
Closed
b
Closed
c
Transition
d
Open
0
-1
-2
-3
-4
-5
log H+ pressure (nPa)
2
1
0
-1
-2
-3
-4
-5
Plasma Beta (log scale)
-70
-35
0
35
70
105
90
45
0
-45
-90
Z
X

Figure 3.4 The logarithm of the H^+ pressure and of the plasma beta in the XZ plane at solstice are shown in the left and right column, respectively. Both color bars are displayed at the top right corner. The magnetic field lines are represented in yellow in the left column, and the red arrows represent the direction of the magnetic field. The labels at the far left indicate if the global configuration of the magnetosphere is closed, open or transition between closed and open. This figure displays the first half of the planetary rotation period.

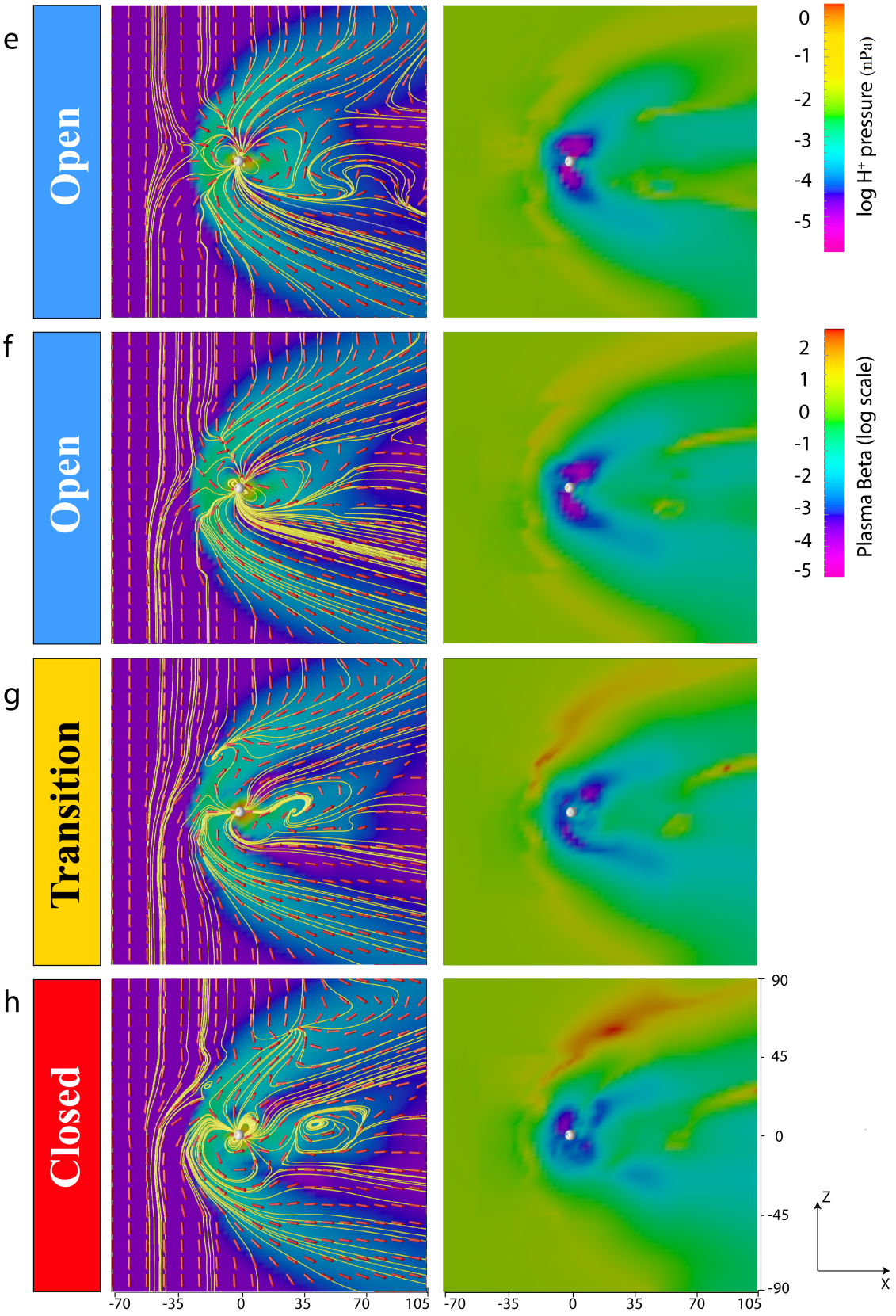
e
Open
f
Open
g
Transition
h
Closed
0
-1
-2
-3
-4
-5
log H+ pressure (nPa)
2
1
0
-1
-2
-3
-4
-5
Plasma Beta (log scale)
-70
-35
0
35
70
105
90
45
0
-45
-90
Z
X

Figure 3.5 The logarithm of the H^+ pressure and of the plasma beta in the XZ plane at solstice are shown in the left and right column, respectively. Both color bars are displayed at the top right corner. The magnetic field lines are represented in yellow in the left column, and the red arrows represent the direction of the magnetic field. The labels at the far left indicate if the global configuration of the magnetosphere is closed, open or transition between closed and open. This figure displays the second half of the planetary rotation period.

3.4.2 Solstice Case

In this section, we will discuss the simulation of Uranus' magnetosphere during the solstice season, by using the physical parameters discussed in the methodology section. Aside from modifying the direction of the solar wind incidence relative to Uranus to reflect the solstice season, all other parameterizations were kept the same. Similarly to the previous section, in Figure 3.4 and Figure 3.5 we show the revolution of the global magnetosphere over one rotation period during solstice. The left panels show total plasma pressure and the right panels show plasma beta again to illustrate where reconnection-favorable plasma beta is spatially correlated to reconnection-favorable magnetic alignment. Rows (a) – (h) display the magnetospheric geometry with eight even intervals in one Uranus day, starting after the model reaches steady state.

Row (a) reveals that a dayside reconnection occurs near the polar region in the northern hemisphere as well as tailward along the southern magnetopause flank. Though this high latitude reconnection is occurring, the overall structure of Uranus' magnetic field is that of a closed magnetospheric configuration [Lu et al., 2013]. On the night side there are two reconnection regions. They exist at high latitudes in the magnetotail, along putative plasmasheet locations which rotate in and out of the image's XZ plane, and occur where the plasma beta is locally high relative to the surroundings. Again, we note that the plasma

beta inside the magnetosphere is generally very low as Uranus' magnetosphere is magnetic field dominated, except in the plasmasheet(s) and along the magnetopause boundary. Uniquely for a planetary magnetosphere, Uranus is believed to posses a curved current sheet because of its tilt angle [Schulz et al., 1996]. In row (b), 1/8 Uranus day later, we observe that the location of northern dayside reconnection at the magnetopause is moving closer to the ecliptic plane, together with the magnetic polar region of the rotating planet. The night-side reconnection from the northern hemisphere shifts to the distal tail (far right edge of the frame) as the closed magnetic field region in the magnetotail expands downstream. Correspondingly, the plasma beta decreases planetward of 100 R_u in the tail, and hence provides reconnection stable conditions only along the magnetopause and far downstream. As the magnetic pole continues its precession toward the ecliptic, the plasma beta near the sub-solar point increases, which suggests even more favorable conditions along the dayside magnetopause for reconnection through this phase of the rotation. In row (c), the magnetic field of Uranus on the dayside is perpendicular to the IMF, the interaction between Uranus' magnetic field and the IMF is complicated because there are no parallel or anti-parallel components between them in the meridian plane. Additionally, there is a local increase in the plasma beta near the sub-solar point during this critical time when the dayside magnetic field changes from parallel to the IMF to anti-parallel to the IMF. This is the threshold past which the magnetosphere transitions from a closed magnetosphere to an open magnetosphere. We call this "switch on" [Cao and Paty, 2014, 2015]. Row d reveals that the magnetic field component antiparallel to the IMF is increasing and thus the sub-solar point reconnection starts to occur. Rows b and d are asymmetric likely due to the dayside reconnection effect on the magnetosphere.

Row (e) features the magnetic field component antiparallel to the IMF reaching maximum. At this point, the global magnetosphere of Uranus is considered to be an open magnenetosphere, which is almost reconnection driven, and there is a Dungey Cycle-like process in the magnetosphere. The current sheet might not develop a full stretching due to the interruption of the planet's rotation [Voigt et al., 1987]. The relatively high plasma beta regions on the day-side and night-side become thicker. In row (f), the polar region is moving back to the ecliptical plane. The relatively high plasma beta region in the night side shrinks, which might be because the rotation drives the high plasma beta region out from this plane. Row (g) shows the second time when the magnetic field of Uranus on the dayside is perpendicular to the IMF. The relatively high plasma beta region on the night side remains small but that on the dayside is increasing in high latitude of the northern hemisphere, which indicates that a high latitude reconnection starting to form. The global magnetospheric structure tends to be closed. This is the process that distinguishes between an open magnetosphere and a closed magnetosphere, which we call "switch off". Row (h) illustrates that the polar reconnection forms again in the northern hemisphere. We observe that the plasma beta on the day side in the northern hemisphere is higher than that of the southern hemisphere because of the high latitude reconnection. The region of high plasma beta on the night side remains small at this time until the start of the following rotation period. Figure 3.4 and Figure 3.5 show that dayside reconnection plays a very important role in the global magnetospheric structure and in modulating the plasma beta relative magnitude and distribution on the global scale, which results in the high gradient of plasma beta to impact the reconnection formation [Masters, 2012, 2015]. Uranus, during both

equinox and solstice, has similar “switch-like” magnetospheric processes which drive the global magnetosphere to transition between open and closed structure.

The level of asymmetry of Uranus’ magnetopause is larger than that of Saturn's [Masters, 2015]. Our results show such an asymmetric characteristic by plasma beta spatial distribution and by the global magnetic configuration. The possible factors resulting in this asymmetry may include 1) the reconnection region’s influence near the magnetopause; 2) planetary rotation making a difference between the southern and northern hemispheres; 3) the natural asymmetry caused by the oblique rotation axis. The third factor is also the major reason for asymmetry inside the magnetosphere. The high plasma beta regions with steep gradients provide favorable conditions for magnetic diffusion and are responsible for the magnetic shear necessary to enable local reconnection.

The previous sections describe the importance of Uranus’ rotation in determining the frequency and location of reconnection in the magnetosphere due to the OTD and Uranus’ high obliquity. This rotation and reconnection also plays an important role in determining the overall structure of the magnetosphere, specifically the current sheet in the magnetotail. Figure 3.6 illustrates a time sequence over the course of one Uranus day of a slice through the magnetotail in the YZ plane at 50.4 R_u downstream from Uranus during solstice conditions. The view is from upstream, looking past Uranus at the slice through the tail, and mapped on that slice is the proton pressure sourced from the solar wind and the ionosphere. The current sheet orientation relative to the YZ plane can be seen to rotate consistently with the rotating orientation of the magnetic axis (which is shown projected in the YZ plane in the inset next to each snapshot in time). The orientation of the plasmasheet does appear to lag behind that of the magnetic axis, and is curved rather than simply

perpendicular across the magnetotail relative to the magnetic axis. This curved plasmasheet structure is related to the combination of OTD and solar wind interaction stretching the tail asymmetrically as the dipole orientation precesses about the rotation axis. The current sheet is not only curved but is also twisted with increasing distance from the planet, lagging further behind the magnetic axis at greater distances down the magnetotail. In Figure 3.6, the asymmetry of the current sheet thickness close to the magnetopause boundary is shown to decrease from T=2.25 Uranus day to T=2.5 Uranus day (where both edges of the magteotail are similar in thickness), and increases from T=2.5 Uranus day to T=3.0 Uranus day, where T is modeling time in the simulation. The largest asymmetry is achieved at T=3.0 Uranus day and the smallest asymmetry is at time T=2.5 Uranus day. We found that the period of the variation of asymmetry of the current sheet is consistent with the planetary rotation period over several rotations, which is probably due to periodic reconnection and the resulting convection in the magnetosphere. The shape of the lobes' cross section at T=2.5 Uranus day is different from that at T= 3.0 Uranus day. This is possibly because of the large magnetic tilt and stretching of the tail during rotation [Schulz et al., 1996]. The areas of the two lobes are also unequal with the larger one being about 1.5-2 times the area of the smaller one at this distance.

Behannon et al. [1987] revealed a curved tail current sheet, which was also asymmetric in thickness between dawn and dusk, by investigating the partial crossing of the current sheet by Voyager 2. The dipole tilt angle fluctuates back and forth between 38.9° and 23.1° relative to the Z axis over the planetary rotation. This is related to the formation of the curved current sheet, but the mechanism by which the asymmetric structure formed is ambiguous. Voigt et al. [1987] raised the same question and speculated

that it might be either the result of time variations or a structural signature of the magnetotail. They stated that an open magnetosphere of Uranus can result in a highly asymmetric tail plasma sheet by considering the interaction with the IMF [Voight et al., 1983]. This agrees with our model which links reconnection with the IMF and the variation of the asymmetric tail current sheet. Figure 3.6 shows that the asymmetry of the current sheet might be not only structural for the magnetotail but also varies with the rotation period. The two structural factors in our model are the dipole tilt and the periodic reconnection with the IMF, of which the former probably dominates the curvature of the plasma sheet [Schulz et al., 1996] and the latter thus might be the factor to affect the asymmetric structure of the current sheet. Furthermore, the periodic interruption of the convection process might be associated with other magnetospheric activities such as periodic substorms [Voigt et al., 1987].

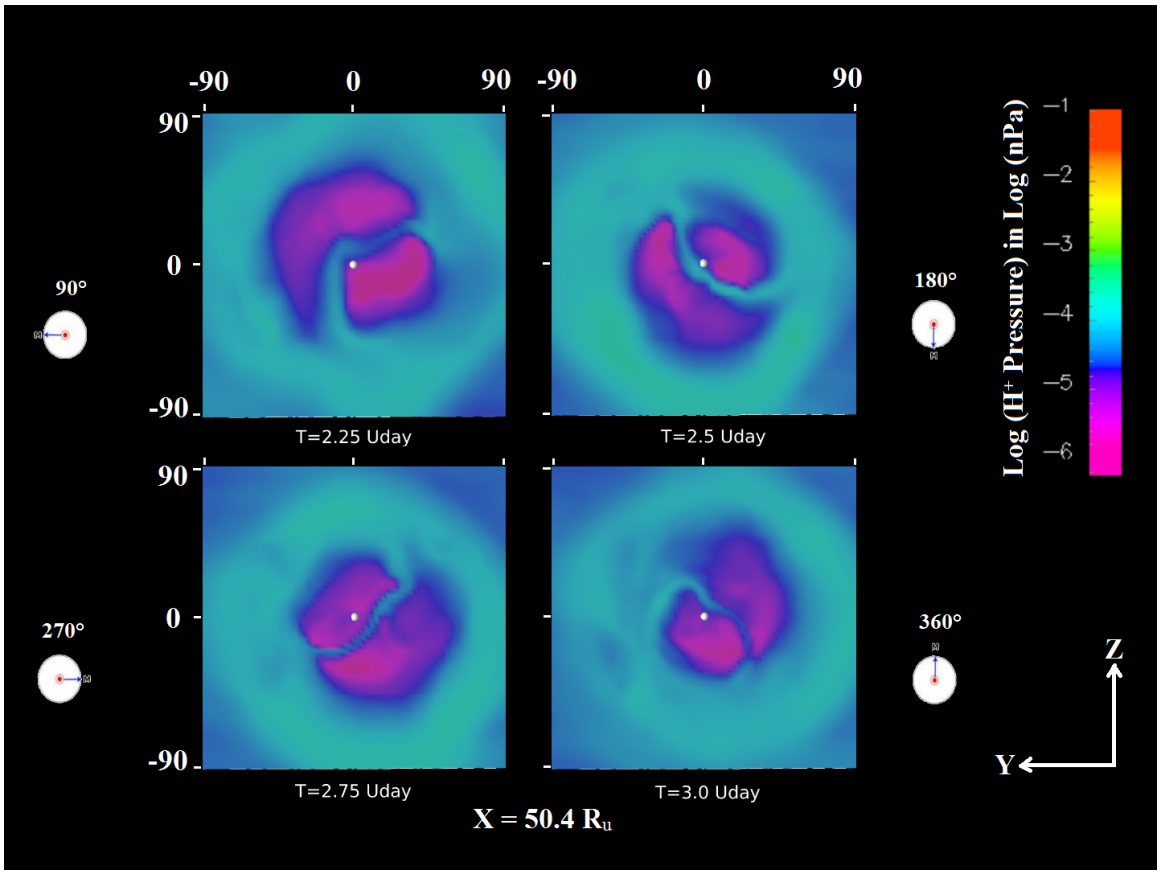

Figure 3.6 The plasma pressure of protons sourced from both solar wind and ionosphere for four different times on the cross section (YZ plane) with a distance of 50.4 R_u downstream. The white sphere in the center of figures represents the projection of the planet on the YZ plane. The clock angle on the side shows the projection of the magnetic axis on the YZ plane. The red spot in the center of the circle points to the Sun.

3.5 Conclusion

The Voyager 2 spacecraft observed Uranus' magnetosphere and quantified its defining characteristics. We developed a generalized version of our Multifluid MHD model of Uranus' magnetosphere to simulate the global magnetosphere for solstice and equinox seasons. Our model successfully simulated Uranus' high obliquity, large tilt angle between the rotation axis and magnetic axis, and off-centered dipole moment. Our simulation revealed that the magnetospheric variation is dependent on diurnal rotation and seasonal

azimuth. We investigated the existence of a "switch-like" magnetosphere during both solstice and equinox seasons and demonstrated how the open magnetosphere transitions to a closed magnetosphere and vice versa. The results showed that reconnection plays an important part in this process. The plasma beta on a global scale showed that the magnetosphere is generally magnetic field dominant, except for some local structures such as reconnection regions and the magnetosheath. The cylindrical symmetry of the magnetosphere is broken by both the magnetic dipole tilt relative to the Z axis and the periodical variation of the interaction between the planetary field and the IMF. This periodic evolution of the magnetosphere includes a variation of the dawn-dusk asymmetry of the current sheet, which is modulated by the planetary rotation. We conclude that the variation about this asymmetry might be associated with the interaction with the IMF on the dayside which likely dominates the convection process throughout the magnetosphere. The possibility that solar-wind-driven magnetospheric convection might result in periodic substorms is also an interesting question [Voigt et al., 1987] and will be studied in our future work. Our results indicate that the multifluid model is remarkably adept at reproducing the characteristics of the Uranian magnetosphere, especially with respect to studying global and local structures such as the asymmetric evolution of the current sheet. Our model is generally applicable to studying the ice giant planets and analogous exoplanets, and can be utilized for Neptune-Triton's magnetospheric system and exoplanet system in the future.

CHAPTER 4. DIURNAL AND SEASONAL VARIABILITY OF URANUS' MAGNETOPAUSE UNDER DIFFERENT IMF

4.1 Summary

We investigated the diurnal and seasonal variations of the magnetopause boundary under different Interplanetary Magnetic Field (IMF) orientations. We implemented our multifluid magnetohydrodynamic (MHD) model of Uranus' magnetosphere [Cao and Paty, 2017], in combination with Voyager 2 observations, to simulate and predict the variability of magnetospheric boundaries. We quantitatively analyzed Uranus' magnetopause in terms of the subsolar standoff distance the flaring parameter and tracked the variation in cusp indentation as these parameters varied as a function of rotation, seasonality, and IMF variation. The study demonstrated the asymmetry of the magnetopause is highly dependent on the rotation of Uranus under specific IMF orientations. The shape of the magnetopause is also affected by the off-centered dipole moment.

4.2 Introduction

Voyager 2 spacecraft flew by Uranus in 1986 and made in situ observations at Uranus' solstice season, when the planetary rotation axis was approximately pointed towards the Sun. However, due to the large obliquity, Uranus' rotational axis relative to the solar wind direction varies greatly from solstice to equinox. As Uranus' orbital period is 84 years, 21 years after the Voyager 2 spacecraft encounter the rotation axis moved from nearly antiparallel to perpendicular to the direction of the Sun, as the planet approaching the equinox. Therefore, the seasonal variation of the rotational geometry relative to the

upstream solar wind results in distinct magnetospheric configurations at different seasons [Cao and Paty, 2017]. In the post-equinox era, auroral emissions on Uranus were observed using Hubble Space Telescope (HST); these emissions revealed a unique latitudinal distribution compared to other planets [Lamy et al., 2012, 2017]. The structure of the cusps at Uranus have not been explored in previous studies, and may prove to be an important region affecting auroral morphology and intensity. While Cao and Paty [2017] examined seasonal effects on reconnection at Uranus, several questions related to magnetospheric variability and its response to the IMF were not yet addressed. For instance, how does the overall magnetopause shape (e.g. stand-off distance, flaring parameter) evolve with planetary rotation under different IMF orientations, and what is the resulting effect on the depth and location of the cusps.

The study of Uranus' magnetosphere has gained attention in recent years due to its unique magnetic and rotational geometry in our solar system. Uranus has a large obliquity, a highly tilted and off-centered dipole moment. The interaction with the solar wind results in a highly asymmetric and dynamic magnetosphere, which has not been observed at other planets. The location and shape of magnetopause reflects the complex interaction of the magnetosphere with the incoming solar wind. The magnetopause is sensitive to dynamic pressure of solar wind and the orientation of IMF and is susceptible to Kelvin–Helmholtz (KH) instability, as it is an important transition region for the momentum and energy of the particles from the solar wind to the magnetosphere [Ma et al., 2017] [Master, 2017]. Masters [2014] used an analytic model to investigate the variation of the reconnection favorable condition on the magnetopause with the planetary rotation and IMF orientation by assuming the magnetopause surface as a parabolic conic section. Cao and Paty [2017]

used a multifluid MHD model to reveal that Uranus has a "switch-like" magnetosphere which opens and closes alternatively every planetary rotation and periodic reconnections occur on the dayside magnetopause boundary. However, detailed and quantitative study of variable topology of the upstream magnetopause of Uranus has not been performed. This is due to both a lack of in situ spacecraft data and the fact that there have been few generalized numerical simulation for Uranus' global magnetosphere examining seasonal variability until recent years [Cao and Paty, 2017, Griton, et al., 2018]. Mejnertsen, et al., [2016] also used a numerical model to simulate the magnetopause of another ice giant Neptune. Scientists have developed some geometric models to describe the magnetopause shape of other planets such as Earth [Lu et al., 2013] and Mercury [Winslow et al., 2013] by fitting an analytical function form with the spacecraft data. We adopt a similar method, modified and applied to studying the diurnal and seasonal variations of Uranus' magnetopause asymmetries as predicted by our multifluid MHD simulation. In this paper, we will use the results of our global simulation combined with the streamlines method [Palmroth et al. 2003] to figure out the shape and location of Uranus magnetopause boundary. We will then use the analytical function form [Shue et al., 1997; Lin et al., 2010] to measure its axial asymmetry. Our investigation indicates that the variation of magnetopause structure is dominated by the planetary rotation at specific season and IMF. The structures of the magnetopause at different seasons are largely different due to the distinct rotational and magnetic geometry relative to the upstream solar wind.

4.3 Methodology

Our numerical model is developed based on the multifluid MHD (Magnetohydrodynamics) model [Winglee, 1998], which is used to study the interaction

between the solar wind and the planetary global magnetospheres. This model has already been used to study different planetary magnetospheres and the interaction between the magnetosphere of the planets and their icy moons. For instance, they are Earth's magnetosphere [Winglee, 1998], Ganymede's magnetosphere [Paty and Winglee, 2004, 2006], and the Saturn's system coupled with Titan [Winglee et al., 2009]. Our model takes into account separate fluids for electrons and different ion species, of which the details were discussed in [Cao and Paty, 2017]. Our model can exclusively track the solar-wind-sourced fluids and study how the magnetopause responds to the solar wind and the planetary rapid rotation. The coordinate system of the model is centered at Uranus, in which the X axis points away from the Sun, the Y axis lies in the orbital plane and parallels to Uranus' orbital velocity, and the Z axis completes the right-handed system. We use a nested grid system in our model, which assigns the outermost boundaries from -100 R_u upstream and +124 R_u downstream in the X direction, and ±128 R_u respectively in the Y and Z directions. By analyzing Voyager 2's magnetometer (MAG) data [Xue et al., 1996, Lepping et al., 1989, Cao and Paty, 2017], we set the IMF to be 0.1 nT strength in the model. In order to study the response of the magnetopause to the IMF orientation, we set IMF respectively southward (-Z direction), eastward (-Y direction) and zero (no specific direction). The initial setup of planetary rotation and inner boundary condition has been discussed in our previous paper [Cao and Paty, 2017].

In order to analyze the magnetopause structure of Uranus, we used an automated technique based on the streamlines to identify the magnetopause boundary like Palmroth et al. [2003]. A set of streamlines is initialized at X = -50 R_U, far outside the bow shock. The streamline grid is defined in the YZ plane in a 96*96 R_U box with the X axis at the

center, on which the streamline starting points distributes equally along each axis, giving in total 3721 streamlines. When the set of streamlines is mapped towards downstream, the magnetopause boundary is automatically identified by searching a threshold void of streamlines starting from the X axis like Palmroth et al. [2003].

Shue et al. [1997, 1998]'s analytic model describes the magnetopause shape by the stand-off distance and the flaring parameter. It has been successfully applied to different magnetopauses such as Earth's [Shue et al., 1997; Liu et al., 2012], Saturn's [Arridge et al., 2006], Mercury's [Winslow et al., 2013, 2017]. However, the model simply assumes the magnetopause shape is symmetric about the X axis. In order to quantitatively measure the asymmetry of the magnetopause, the azimuth angle was introduced in the model. The equation is defined as below:

$$r = r_{SS}\left(\frac{2}{1+\cos\theta}\right)^{\alpha(\psi)}$$

where r is the distance from the planet, r_{SS} is the subsolar magnetopause distance, θ is the angle between the magnetopause point and the X axis, α is the flaring parameter, and ψ is the azimuth angle, which means the flaring parameter is a function of the azimuth angle. The flaring parameter indicates if the magnetotail is closed ($\alpha < 0.5$) or open ($\alpha \geq 0.5$). For the sake of investigating the north-south and east-west (dusk-dawn) asymmetry, azimuth angle ψ is respectively set to be 0°, 90°, 180°, 270°. Using the analytic model fits our simulation results extracted by the streamline method, we obtained the flaring parameter of magnetopause in different hemispheres at the sequential rotational phases above for different seasons.

Another important structure of the magnetopause is the cusp indentation or the cusp depth. This region is associated with the open and close boundary of the magnetic field lines sourced from the surface of the planets, and is the main area where the energetic particles precipitate into the ionosphere. A large amount of aurora emission events are associated with this region. The morphology of the cusp indentation is very important for modulating the dayside magnetopause structure and for studying the entry of the momentum and energy from the solar wind into the magnetosphere. We determine the cusp indentation using the method discussed in Zhong et al., 2015, comparing the MHD model results with the analytical fitting results.

4.4 Results

As we discussed above, for the most of planetary magnetospheres, the magnetopause boundary plays a significant role in the interaction with the solar wind. Studying the magnetopause geometry is essential to investigate the mass, momentum and energy transportation/interchange between the solar wind and the magnetosphere. Compared to other planets, the situation at Uranus is more complicated as it possesses an off-centered, largely tilted magnetic dipole moment, which is fixed at a rapidly rotational axis with a highly obliquity. The variability of the global magnetosphere structure of Uranus has been studied recently using a numerical simulation, based on Voyager 2's measurement [Cao and Paty, 2017]. In this paper, the bulk of our work will focus on diurnal and seasonal variations with respect to the magnetospause configuration, using the combination of an analytic method and the numerical simulation results.

To investigate the effect of IMF orientation on the magnetopause structure, we simulated the magnetosphere of Uranus respectively at solstice and equinox season in terms of three different IMF orientations. They are southward, eastward and zero in magnitude. The Voyager 2 spacecraft measured the average orientation of the IMF before its encountering is southward [Cao and Paty, 2017]. The eastward orientation is based on the Parker's model [Parker, 1958]. We set zero magnitude for the IMF to compare the response of the magnetosphere with and without the impact of the IMF. Besides, for a certain amount of period, the average magnitude could be assumed to be close to zero.

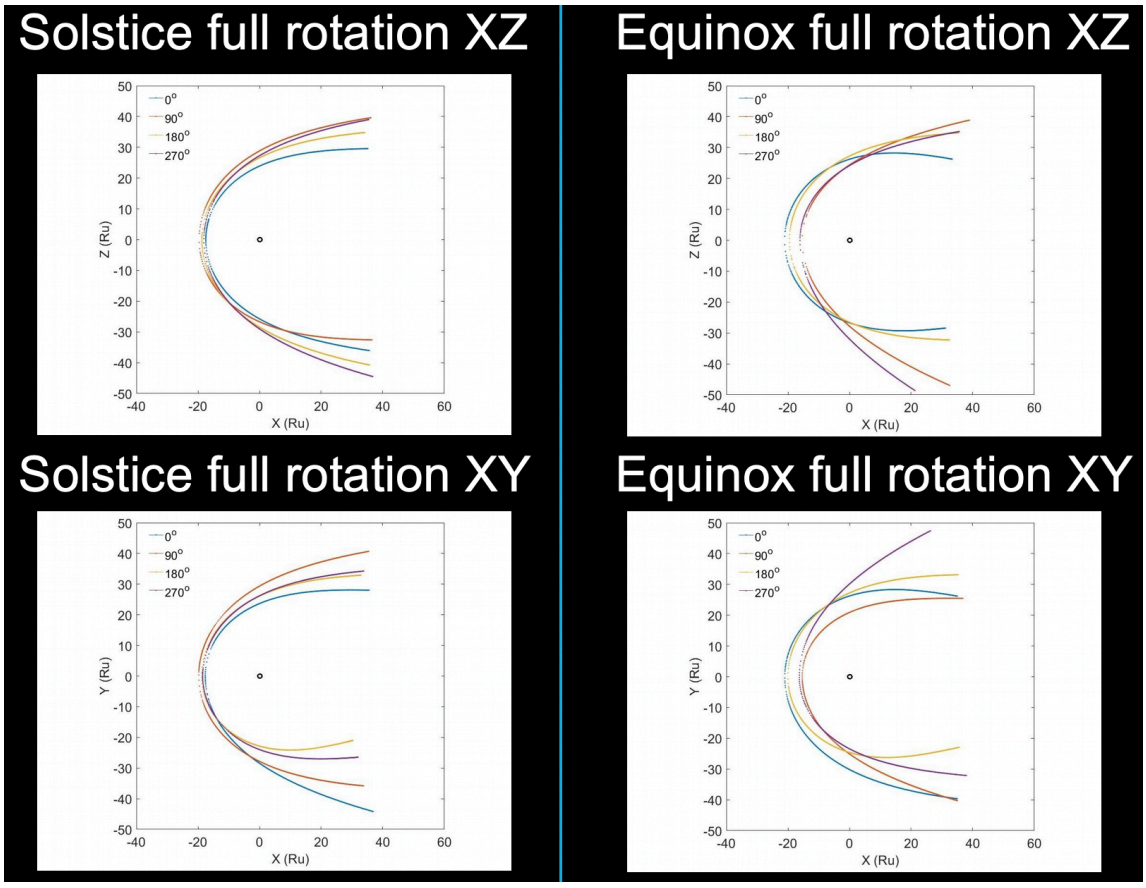

Figure 4.1 The variability of magnetopause during one Uranus day respectively at solstice and equinox under southward IMF, using the analytic method we discussed. Blue, red, yellow, purple color respectively represents four different rotational phase: 0°, 90°, 180°, 270°.

How the magnetopause dynamically react to the planetary rotation under different IMF orientaion has not been clear so far. One feasible method is to learn it from the simulation results based on Voyager 2's measurement. Cao and Paty [2017] demonstrated that the planetary rotation dominates the global configuration of the magnetosphere when Voyager 2 encountered Uranus (at solstice) and at equinox, under the condition of the southward IMF. The rapid rotation controls the paces of Uranus' magnetosphere dancing between "open" and "closed". The southward IMF determines which rotational phase the reconnection at the magnetopause occurs at. In this section, we will further study the subtle structures of the magnetopause based on the global results to figure out how the magnetopause delicately response to the variation of the solar wind in different seasons.

The results indicate that the periodic variation of the magnetopause depends on the planetary rotation. Figure 4.1 reveals the variation of the magnetopause boundary fitted by Shue's model. The magnetopause stand-off distances at solstice, as shown in (a) and (b), are very close to each other during different rotational phases, between 18 - 20 R_U upstream from the planet. At this season, the attack angle remains almost the same during planetary rotation, where the attack angle is the angle between the direction to the Sun and Uranus' magnetic dipole orientation. The quasi-static attack angle is determined by the quasi-invariant magnetic geometry of the planet relative to the upstream solar wind because the rotational axis is nearly pointing towards the Sun. In contrast, the stand-off distance at equinox, though, bounces back and forth every 90° of the planetary rotation, as the attack angle at this season is alway changing with a period of half planetary rotation. The flaring parameters in (a) at both hemispheres at 0° are less than those at 180° at XZ plane, which indicates the magnetotail or magnetopause at tail region is more open when the global

structure of Uranus' magnetosphere is open, caused by the dayside reconnection [Cao and Paty, 2017]. The magnetotail at 0° and 180° extends respectively eastward (-Y direction) and westward (+Y direction) on the XY plane, which might be dominated by the inertial effect of the planetary rapid rotation. Similarly, at equinox, as (c) and (d) show, the geometry of magnetotail is more open when the global structure of Uranus' magnetosphere is open with dayside reconnection occurring. The stand-off distances at 0° and 180° are larger than those at 90° and 270°, which results from the larger attack angle at 0° and 180°. The magentotail on the XY plane oscillates between eastward and westward during planetary rotation, as is shown in (d). Therefore, the fluctuation of the magnetopause boundary is driven by the rotational interaction of the planet with the solar wind.

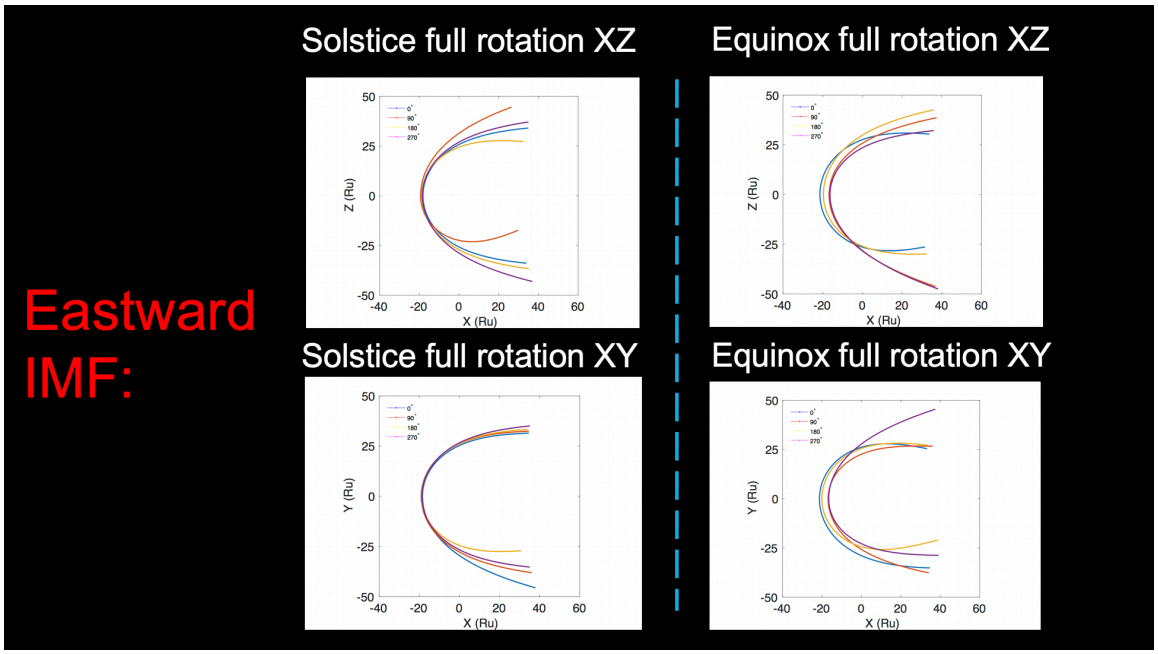

Figure 4.2 The variability of magnetopause during one Uranus day respectively at solstice and equinox under eastward IMF, using the analytic method we discussed. Blue, red, yellow, purple color respectively represents four sequential rotational phases: 0°, 90°, 180°, 270°.

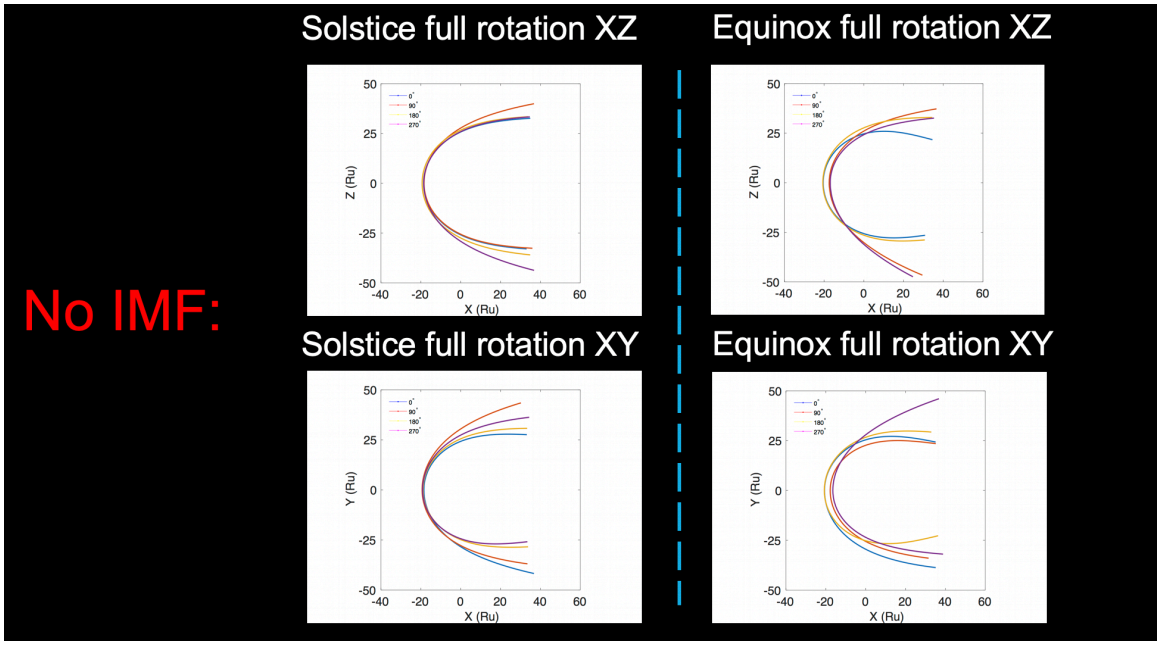

Figure 4.3 The variability of magnetopause during one Uranus day respectively at solstice and equinox without IMF, using the analytic method we discussed. Blue,

red, yellow, purple color respectively represents four sequential rotational phases: 0°, 90°, 180°, 270°.

Figure 4.2 demonstrates the response of the magnetopause to the planetary rotation under the condition of eastward IMF. The magentotail on the XZ plane oscillates between northward and southward during planetary rotation, as (a) shows, which corresponds with the east-west oscillation at XY plane due to the orthogonal orientation of IMF. However, the magentotail geometry under eastward IMF is not as exactly same as that under southward IMF after an orthogonal transformation because of the rotational axis of the planet does not exactly parallel to the direction towards the Sun. Therefore, the X asymmetry of the magnetopause is slightly broken and the slightly varying attack angle affects on the rotational magnetotail to a certain extent. In the condition of zero IMF, as Figure 4.3 shows, the magnetotail geometry is mainly modulated by the planetary rotation, without the influence by upstream IMF which makes the dayside reconnections occur.

At equinox season, the variations of magnetpause geometry under different IMF orientation are similar to each other, as there is no such a quasi-X-symmetry of the rotational axis as that at solstice. The attack angle changes largely during the planetary rotation, which makes the standoff distance from the planet changes significantly with a stable period, even if the IMF remains the same. Compared to Uranus, most of other planets perform a fluctuated standoff distance due to the dynamic solar wind's impact, instead of the effect of their rotation. Therefore, the rotation of Uranus plays a dominant role in the magnetopause geometry, compared to the influence of IMF orientation.

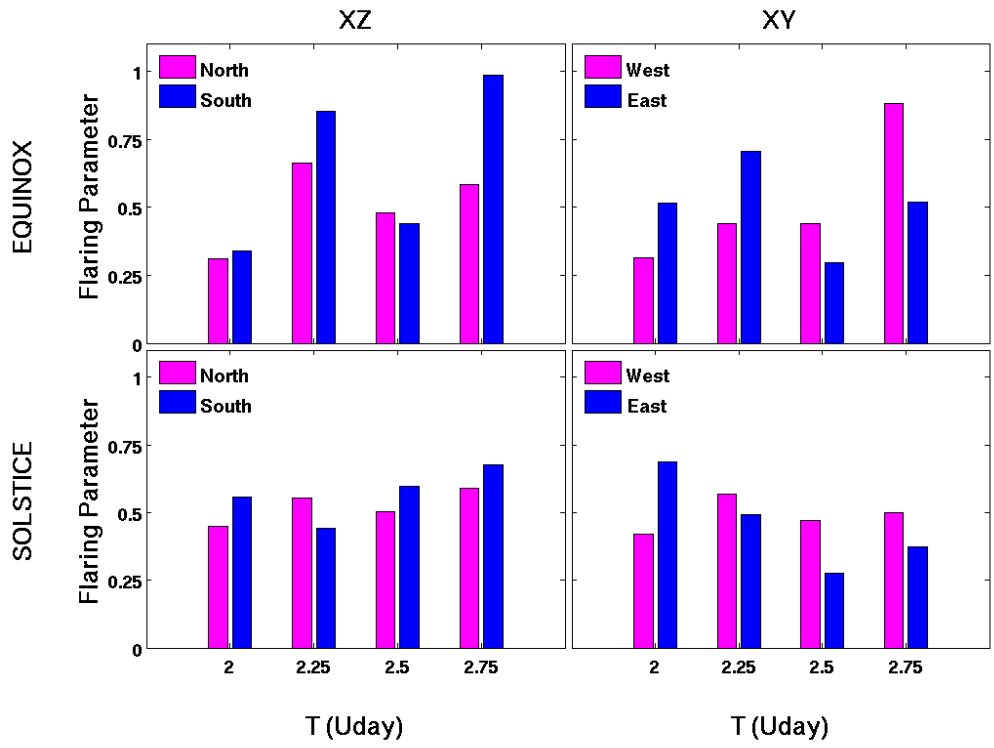

Figure 4.4 The bar plot shows that the variation of the flaring parameter during one Uranus day in XZ (meridian) and XY (equatorial) plane at equinox and solstice season, under southward IMF. The color represents the flaring parameter of different hemisphere. In XZ plane, purple and blue bars respectively represent the flaring parameter of north and south hemisphere, and in XY plane, purple and blue bar respectively represents the flaring parameter of west and east hemisphere.

Figure 4.4 shows the statistics of the flaring parameter during one Uranus day at equinox and solstice respectively in XZ and XY plane, under southward IMF. The overall fluctuation of the flaring is much weaker at solstice than that at equinox during planetary rotation, which is probably due to relatively stable attack angle relative to the upstream solar wind. The more significant fluctuation at equinox is because that the planetary magnetic orientation alternate between pole-on and perpendicular relative to the upstream solar wind. The overall north-south and dawn-dusk asymmetry of flaring is more strongly

expressed at equinox, which is probably resulted from the lack of X symmetry of the rotation axis combined with the off-centered dipole moment on YZ plane. Furthermore, the average flaring parameter oscillates around 0.5 back and forth, which indicates respectively a dynamically open and closed magnetotail. In general, the asymmetry of magnetotail at equinox performs much larger than that at solstice.

In the condition of eastern IMF, that same modulation at equinox dominates the flaring angle signature, but during solstice the flaring angle asymmetry between north and south is enhanced by the presence of the eastward IMF (especially in the XZ plane), which might be due to the non-coplanar relationship between the dipole orientation and the IMF orientation. In other words, the off-center geometry relative to the IMF orientation affects the subtle structure of the flaring asymmetry.

In the condition of zero IMF, the overall flaring of the magnetosphere during solstice is minimized and has the least variability, especially during solstice. The variability at equinox comes from the tumbling of the dipole axis with respect to the solar wind ram direction -- the north and south poles are quite different in strength and alternate during equinox geometry, causing the modulation in the flaring angle.

In general, the variations of the flaring parameter during one Uranus day under different IMF are similar to each other. The main difference under different IMF orientation is their value, as different IMF orientation could modulate the global magnetopause structure through the dayside reconnection, but the planetary rotation relative to the solar wind dominates the general magnetopause shape in the time scale of one Uranus day.

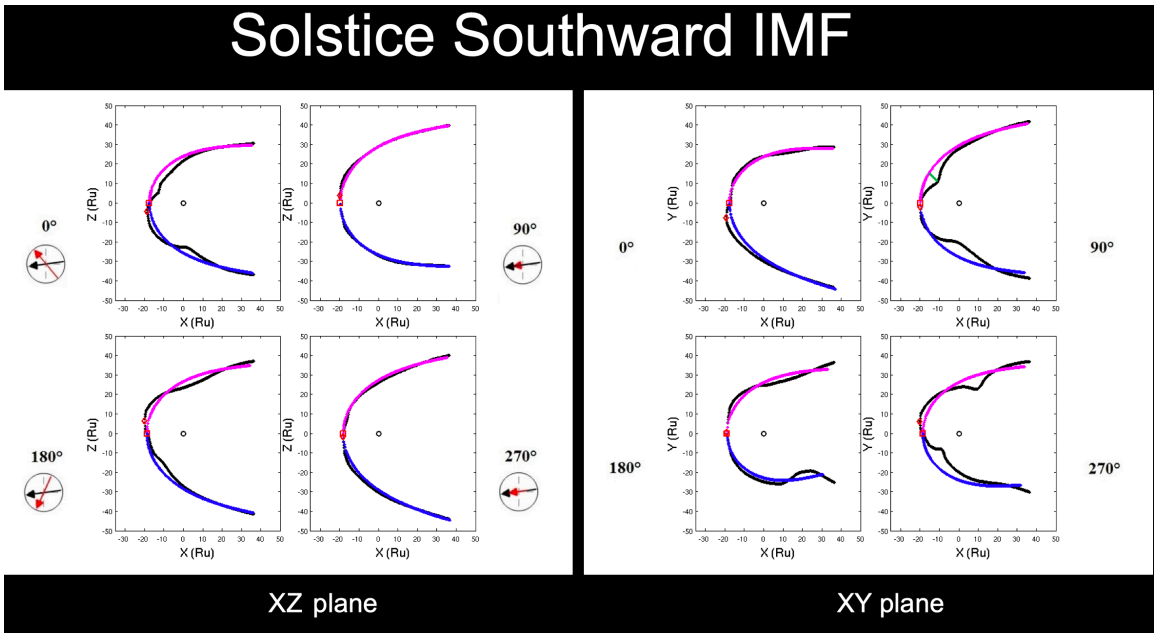

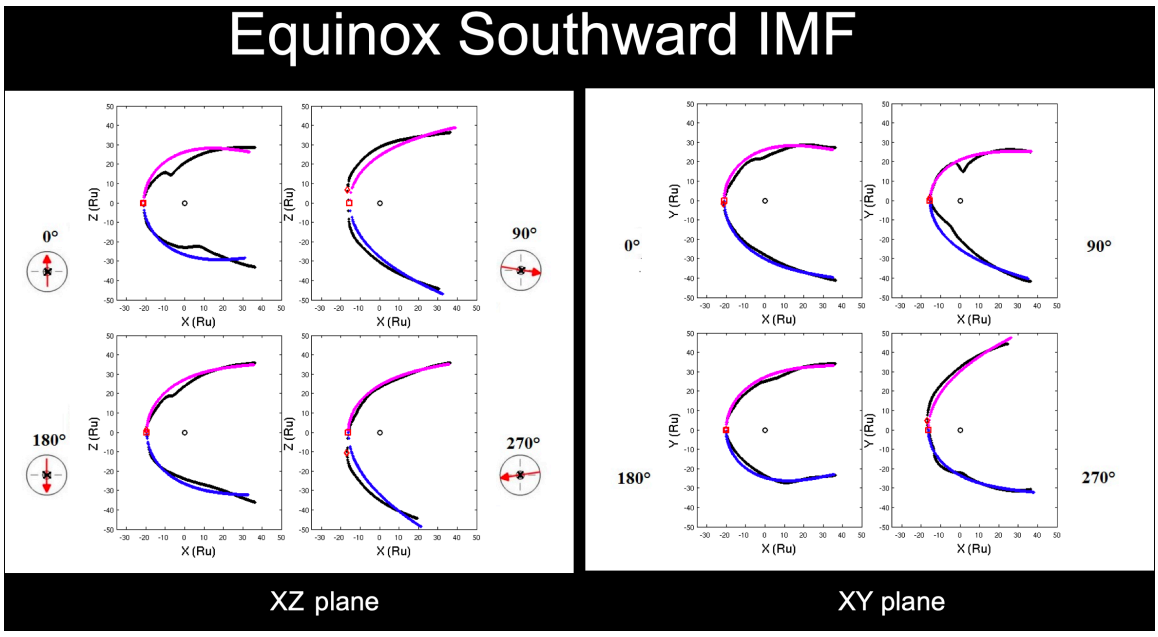

Figure 4.5 This figure shows the evolution of the magnetopause during one Uranus day respectively at solstice and equinox under southward IMF. The black represents the magnetopause result of numerical simulation, the purple and blue represents respectively the magnetopause boundary in each hemisphere from the analytical model we have discussed.

Figure 4.5 displays the comparison of the numerical simulation results and the analytical fitted results. We split the magnetopause fitted results sequentially during one Uranus day, using different color for each hemisphere. The purple and blue represents respectively the magnetopause boundary of northern and southern hemisphere in XZ (meridian) plane, and of western and eastern hemisphere in XY (equatorial) plane. We then superimpose our MHD model results on the fitted results. In order to figure out how the cusp indentation evolves with planetary rotation, we used the method like Zhong et al., 2015, as the discussion section mentioned. In the plane where the cusp appears, we can measure the cusp indentation. We found that the cusp appears alternately in the XZ and XY plane every 90 degree rotation at solstice. This alternation indicates that the cusp rotates along with the magnetic dipole orientation. Besides, the bend of the bulge of the magnetopause changes its direction every half a rotation, which is also due to the adhesion to the rotation of the magnetic dipole with a large attack angle. The cusps at equinox also appear alternatively in the plane of XZ and XY, as the magnetic dipole rotates with a vertical, pole-on, vertical, pole-on scenario relative to the solar wind stream. We found that when the attack angle increases in plane, the cusp indentation in plane increases, and that when the attack angle decreases in plane, the cusp indentation in plane decreases.

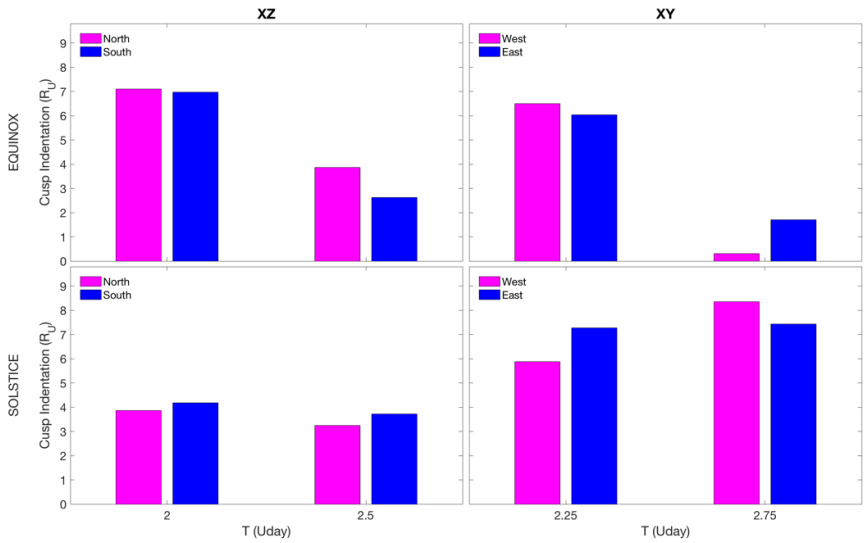

Figure 4.6 The bar plot reveals the variation of cusp indentation during one Uranus at equinox and solstice season under southward IMF. The purple and blue represents respectively the magnetopause boundary in each hemisphere. The vertical axis unit for cusp indentation is R_U.

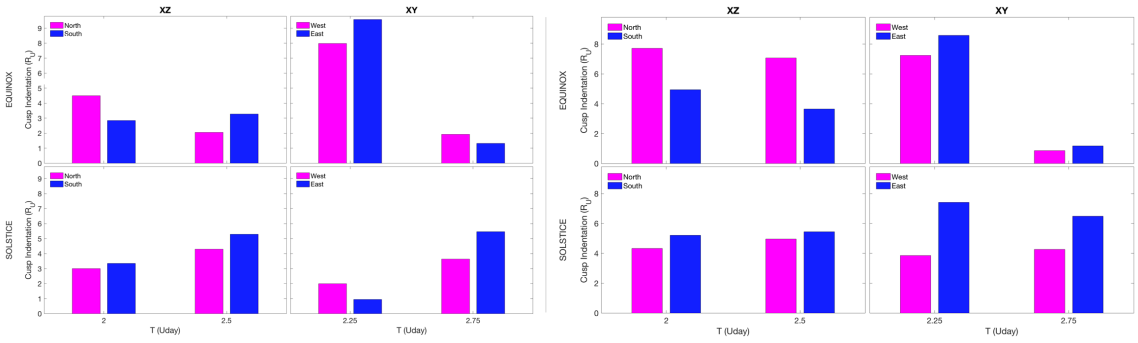

Figure 4.7 The bar plot reveals the variation of cusp indentation during one Uranus at equinox and solstice season under eastward and no IMF. The purple and blue represents respectively the magnetopause boundary in each hemisphere. The vertical axis unit for cusp indentation is R_U.

Figure 4.6 reveals the variation of the cusp indentation with planetary rotation at equinox and solstice seasons, by using bar plots. Figure 4.6 shows that under southward IMF, at equinox season, the depth of cusp indentation differs largely between half a full rotation but slightly between ¼ of a full rotation, which corresponds with the vertical, pole-on, vertical, pole-on scenario of the rotating magnetic field of the planet. In solstice season, the depth of cusp indentation differs slightly between half a full rotation but largely between ¼ of a full rotation. This difference is caused by the change of the rotational and magnetic orientations relative to the upstream solar wind. In XZ plane, at equinox, the cusps indentations at northern hemisphere are larger than that at southern hemisphere. At solstice, the cusp indentations at southern hemisphere are larger than that at northern hemisphere. However, in XY plane, there is no such a rule for the variation of the cusp indentation. This is probably caused by the in-plane reconnection occurring in XZ plane and the global structure being fully closed or open in this plane. In XZ plane, the magnetic field lines near magnetopause are distorted by the southward IMF and westward/eastward magnetic field lines sourced from Uranus, and the cusp region might be modulated by such an interaction.

In the condition of eastward IMF, as the left subfigure of Figure 4.7 shows, the cusp indentation at 2.0 Uranus day in the XZ plane at equinox and 2.25 Uranus day in the XY plane at solstice decrease significantly compared with those under southward IMF condition. This might be because the non-coplane of the magnetic dipole orientation with the IMF orientation such that at these specific rotation phases the deepest indentation of the cusp does not been captured/visualized in the plane. At equinox, the general variations of the cusp indentation at equinox are similar to those in the condition of southward IMF

with interchange the XZ and XY plane, except for that at 2.25 Uranus day, the cusp indentation at east hemisphere is larger than that at west hemisphere. The complex distorted magnetic field interaction combined with the non-coplane of the attack angle might cause this fluctuation. At solstice, the variations at 2 and 2.75 Uranus day are similar to that under southward IMF, which indicates that the rotation and magnetic geometry of the planet mainly dominate the cusp indentation for these phases. But the other half rotation might be more largely modulated by the eastward IMF.

In the condition of zero IMF condition, as the right subfigure of Figure 4.7 shows, the deviation of cusp depth caused by the modulation of the IMF is minimized. Comparing its equinox with the case of southward IMF, the cusps indentation at 2.5 Uranus day is enhanced, which indicates that the dayside reconnection (open structure of global magnetosphere) might deepen the cusp. In the season of equinox, the cusp indentations at 2.25 Uranus day are similar to the case of eastward IMF, rather than that of southward IMF, and the cusp indentations at 2.75 Uranus day are similar to the case of southward IMF, rather than that of eastward IMF, which proved that the modulation effect of the IMF orientation. In the season of solstice, the cusp indentations at 2.25 Uranus day are similar to the case of southward IMF, rather than that of eastward IMF, and the cusp indentations at 2.75 Uranus day are similar to the case of eastward IMF, rather than that of southward IMF. The zero IMF effect seems respectively correspond to half part of the results in the condition of southward and eastward IMF, which indicates that the different IMF orientation modulates the cusp indentation more in some specific rotation phases during one Uranus day.

This reveals how complicated the dynamical and asymmetric magnetopause of Uranus compared to that of other planets.

4.5 Discussion

In this paper, we used the numerical simulation results based on Voyager 2's measurement to study the variations of Uranus' magnetopause during one Uranus day respectively at equinox and solstice season, under the interactions with different orientated IMF. Combined with the analytic fitted method, we investigated the asymmetric structures of the magnetopause by studying the standoff distance, the flaring parameter and the cusp indentations. Such asymmetries include asymmetries in time and space due to the planetary rotation with time.

We found that the standoff distance fluctuates within a small range during one Uranus day at solstice, but fluctuates much larger and bounces back and forth every 90 degree of the planetary rotation at equinox due to the larger periodic variation of the attack angle. Therefore, the magnetic geometry with the planetary rotation relative to the upstream solar wind play a very important role in the variation of the standoff distance.

The second finding is that the flaring parameter, which represent how the shape of the magnetotail is open or closed, is strongly impacted by the rotation of Uranus. By comparing the flaring between northern-southern hemispheres or eastward-westward hemispheres, we can quantitatively measure how asymmetric the magnetotail performs during one Uranus day at different seasons, under different oriented IMF.

The third finding is that the cusp indentations are influenced by all of three factors: the planetary rotation, the magnetic geometry (or different seasons) and the IMF orientation. During one Uranus day, the planetary rotation play a main role in the cusp indentation with a specific magnetic geometry relative to the upstream solar wind, under a specific IMF orientation. During different seasons, the magnetic geometry relative to the upstream solar wind with a specific IMF orientation dominates the variations of the cusp indentations. Finally, the different IMF orientations modulate the cusp indentations at some specific rotation phases at a certain season.

4.6 Conclusion

We investigated the diurnal and seasonal variations of the magnetopause boundary under different IMF orientations, by using the numerical simulation results based on Voyager 2's measurement [Cao and Paty, 2017]. Combined with the analytical fitted model, we quantitatively analyzed the characteristics and variability of Uranus' magnetopause and cusp in terms of the standoff distance, the flaring parameter and the cusp indentation, which helps us to understand the asymmetric structure of the magnetopause and how it varies with the planetary rotation and with different seasons. The results shows the asymmetry of the magnetopause is highly dependent on the rotation of Uranus under specific IMF orientations. The shape of the magnetopause is also affected by the off-centered dipole moment. The variations of the magnetopause are modulated by all of the planetary rotation, the variation of the magnetic geometry and the IMF orientation.

CHAPTER 5. CONCLUSION AND FUTURE WORK

5.1 Summary of the Uranus research

The goal of this dissertation has been to examine the interaction of the distinctive magnetosphere of Uranus with the dynamic solar wind in order to characterize the balance of forces which determine the overall structure and variability of Uranus' magnetosphere. I first developed a description of the internal off centered tilted dipole structure of Uranus based on and validated against the magnetometer observation from the Voyager 2 flyby. I implemented this for the magnetic field boundary condition in a 3-dimensional multifluid simulation of Uranus' magnetosphere under steady southward IMF. This upstream boundary condition was representative of the average conditions during the Voyager 2 encounter. Several rotations of Uranus' magnetosphere were simulated and it was determined that the magnetopause boundary was periodically stable to magnetic reconnection as modulated by the planet's rotation.

Chapter 3 characterized the global interaction of the magnetosphere of Uranus with the solar wind using our multifluid MHD model. The study shows that the rotational and magnetic geometries play a very important role in the configuration of the magnetosphere. The direction of the solar wind velocity and momentum relative to Unranus' magnetic axis varies with the orbital season of the planet, therefore the upstream interaction with the planet during different seasons results in different magnetospheric structures. I verified that a dynamic "Switch-like" magnetosphere exists at Uranus at different seasons which

follows a periodic open-closed-open pattern, by analyzing a large suite of simulations from our multifluid MHD model. The study investigated the evolution on Uranus' magnetosphere and the locations of magnetic reconnection during both solstice and equinox. The simulation confirmed that the high plasma beta gradient regions are usually consistent with locations of large magnetic shear, which combined provide a mechanism for mapping potential reconnection regions. The overall plasma beta distribution described a magnetic field dominant magnetosphere at Uranus. Beyond the magnetopause structure and reconnection periodicity, I also found that the asymmetry of the tail current sheet is dependent on the rotation and off-centered dipole of the planet.

Chapter 4 demonstrated the diurnal and seasonal variations of the magnetopause of Uranus by using the results of the multifluid MHD model along with an analytical shape model to describe the magnetopause as it varied via the dayside magnetospheric interaction with the solar wind. The study used the results of the analytical shape model fit to the MHD simulation to compare the standoff distances in the simulation and in Voyager 2 data, illustrating very good consistency between the plasma dynamic simulation and the data. The flaring parameter extracted from the shape model reveals further details about the asymmetry of this dynamic magnetosphere. This asymmetry varies with the planetary rotation, the season, and the solar wind condition. The cusp indentation also has a similar asymmetry and is an indicator of how the solar wind charged particles gain access to the magnetosphere through the open-closed field line boundary. The cusp indentations are also influenced by three factors: the planetary rotation, the magnetic geometry (or different seasons) and the IMF orientation. In general, the variation of the magnetopause demonstrated the complexity of the interaction of Uranus with the solar wind.

The findings presented in the previous chapters represent significant gains in understanding of Uranus' dynamic and asymmetric magnetosphere; however, several questions remain pertaining to the generation and variability of Uranus' aurora, the interaction of highly asymmetric magnetospheres of the ice giants in general, and the magnetospheric environment such planets provide for their orbiting satellites. This work should prove a useful foundation for further investigations into the ice giant magnetospheric systems. It also lends strong support to future studies of exoplanets, which are heavily populated by ice giant sized planets, and their interaction with the solar wind.

5.2 Continuing Work for Uranus

Our ongoing research on Uranus' magnetosphere work will focus on three aspects. First, the real-time magnetic field data from Voyager 2 will be used in the model instead of the average IMF condition used in our first two studies. This real-time input would provide a more accurate upstream solar wind condition, and a more dynamic varying magnetosphere is expected from the results of the simulation. Second, the precipitation of charged particles into the surface of Uranus will be studied, compared with the structure of the cusp indentation and the aurora emission data. Combination of these parameters can help us deeply understand that how the magnetospheric dynamics effects on the planet. Third, the transitional seasons between solstice and equinox will be investigated by the model. This work will enhance and broaden our understanding of the magnetosphere of Uranus for geometries occurring away from the two 'typical' seasonal extremes. What is the magnetospheric configuration of Uranus and how does it evolve with the planetary rotation during those transitional seasons are still open questions, and ones that are of importance for a possible future mission during 2030 – 2040's.

There are many more questions related to Uranus' magnetosphere which would be interesting to address. For instance, what is the difference of the internal convection of Uranus magnetosphere during different seasons? How does it depend on the seasonal variability? What is the role of the reconnection in the tail dynamics? What is the relationship between the cusp structure and the aurora emission? While our simulation is able to investigate them in more detail, we leave this to future researchers as a more complete observational data set will be needed to fully constrain the questions and benchmark the simulation in greater detail.

5.3 Future Work for Neptune and Triton System

Besides Uranus, I plan to investigate the magnetosphere of the solar system's other ice giant, Neptune. As Neptune has a high obliquity (approximately 28°) and a large dipole tilt angle (approximately 47°) which is to some extent similar to Uranus, the magnetosphere of Neptune is one of our next targets of study. Figure 5.1 shows the preliminary results of Neptune's magnetosphere in XZ plane at the solstice season by using our model. The contour reveals the plasma beta distribution and the yellow lines represent magnetic field lines. I will continue to investigate the diurnal and seasonal variability of Neptune's magnetosphere under different IMF condition.

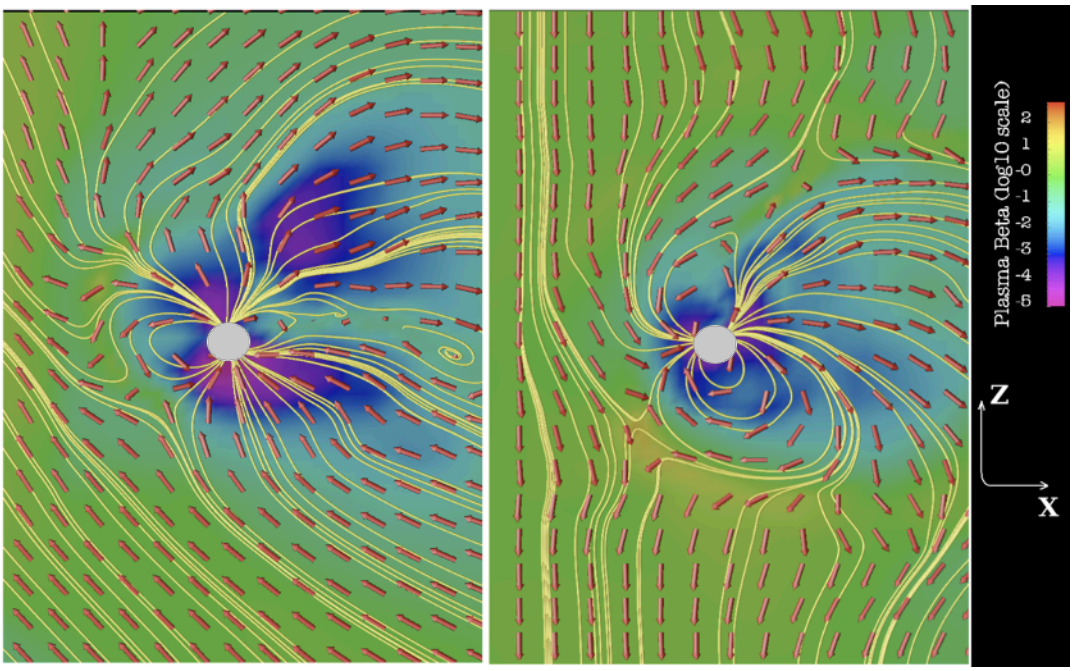

Figure 5.1 Preliminary simulation of the magnetosphere of Neptune during one planetary rotation at solstice by using our multifluid MHD model. The IMF condition varies in the simulation. The IMF orientation in the left panel is northward with a negative X component of the equal strength. The IMF orientation in the right panel is southward. The magnitude of both panel are 0.1 nT.

Moreover, the moon Triton will be embedded into the model in order to study how the overall Neptune-Triton system evolves with the planetary rotation. The Triton has active geysers of nitrogen gas, dark particles and a diffuse atmosphere and might be an oceanic world. How Triton experiences the dynamic and asymmetric magnetosphere of Neptune is very important to study its potential habitability, and the neutrals provided to Neptune's magnetosphere by Triton's atmosphere and plume activity opens up many questions relating to mass transport from a non-equatorial source of plasma (a definitively unique geometry for exploring such questions).

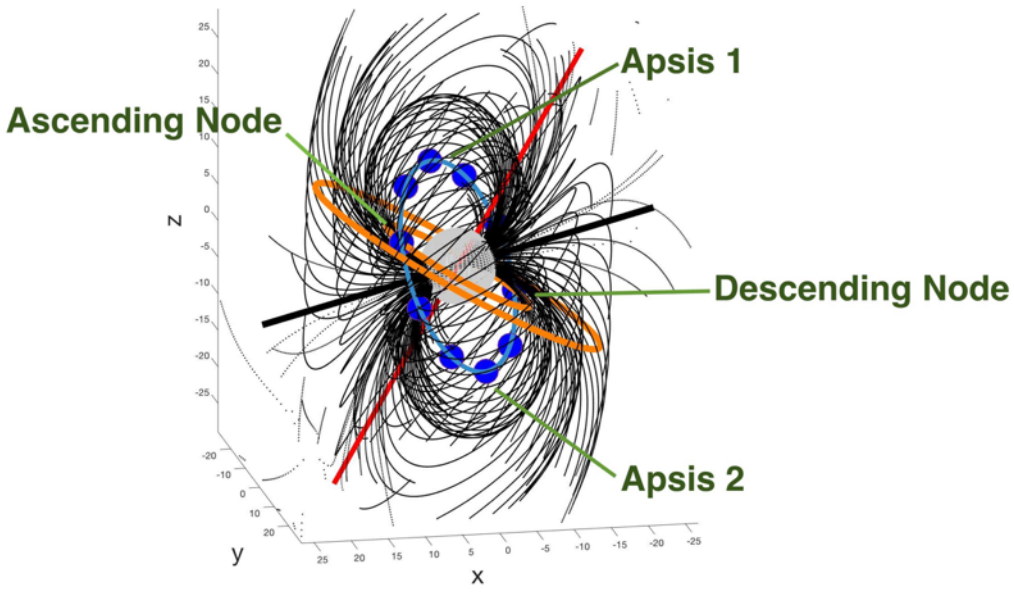

Figure 5.2 The rotational and magnetic geometry of Neptune-Triton system (Paty and Cao, 2018)

Figure 5.2 demonstrates the preliminary analytical model results for the Neptune and Triton system. The red straight line represents the rotation axis of Neptune. The black straight line represents the magnetic dipole axis of Neptune. The orange represents the rotational equator. The grey large sphere represents Neptune. The blue small spheres represent the different locations of Triton in its orbit, four typical locations of which are marked in the figure. The sizes of Neptune and Triton are not to scale. Triton would experience much more complex magnetospheric environment than the moon of other planets. For instance, Triton might cross the high magnetic latitude and low magnetic latitude during the rotation of Neptune.

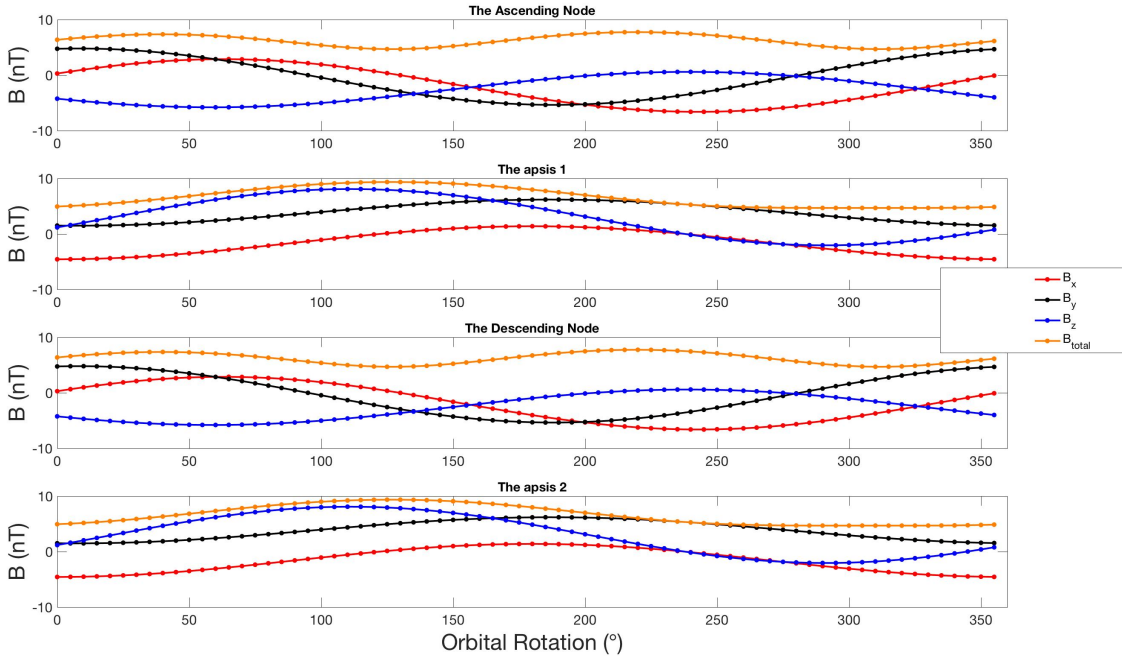

Figure 5.3 The non-offset dipole field during one Neptune's rotation

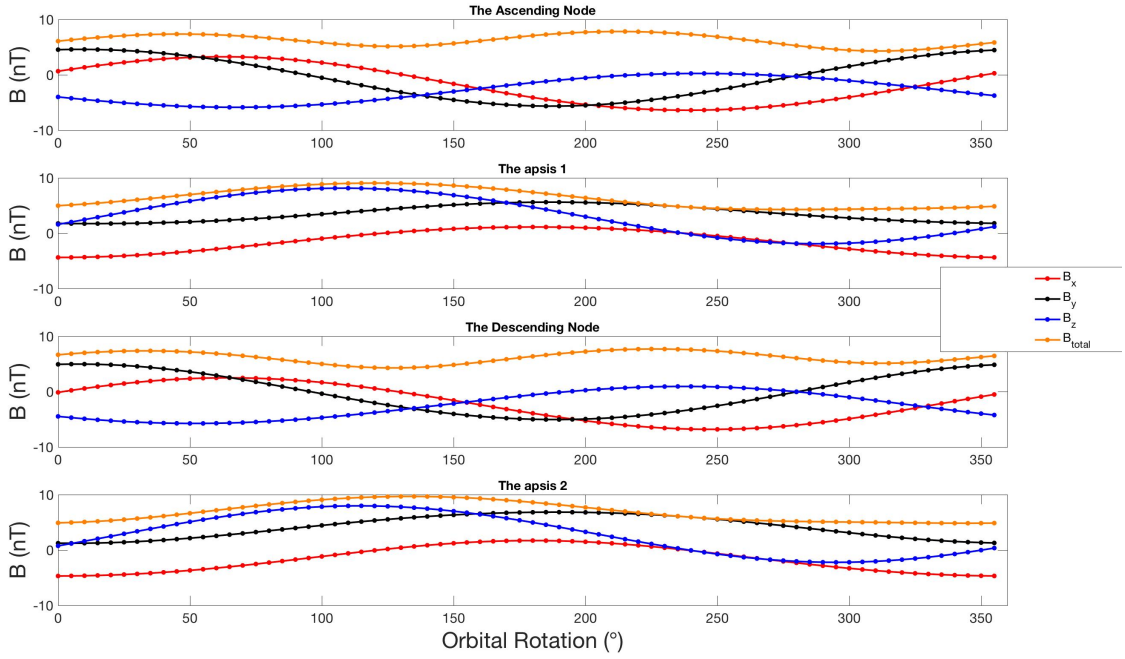

Figure 5.4 The offset dipole field during one Neptune's rotation

Figure 5.3 and Figure 5.4 shows the variation of the magnetic field of Neptune at four typical orbital locations of Triton, as shown in Figure 5.2, during one rotation of Neptune, respectively for the centered and off centered magnetic dipole of Neptune. The magnetic field that Triton experiences at different orbital locations are distinct in general, but if assuming that the dipole of Neptune is centered, as shown in Figure 5.3, the magnetic field at ascending node and descending node are the same because of their symmetric orbital locations, so is that at apsis 1 and apsis 2. However, if considering the off centered dipole position, the symmetry of the orbital locations such as ascending node and descending node is broken, and the magnetic field variation is differentiated even if their orbital locations are symmetric. The differences in the magnetic field local to Triton for the off centered versus the centered Neptune dipole case are small, less than 1 nT, however they may be useful in determining and characterizing interior structure such as a subsurface ocean with observations from future missions. Therefore, the consideration of the off centered dipole is very important to investigate the Neptune and Triton system.

5.4 Future Applications to exoplanets

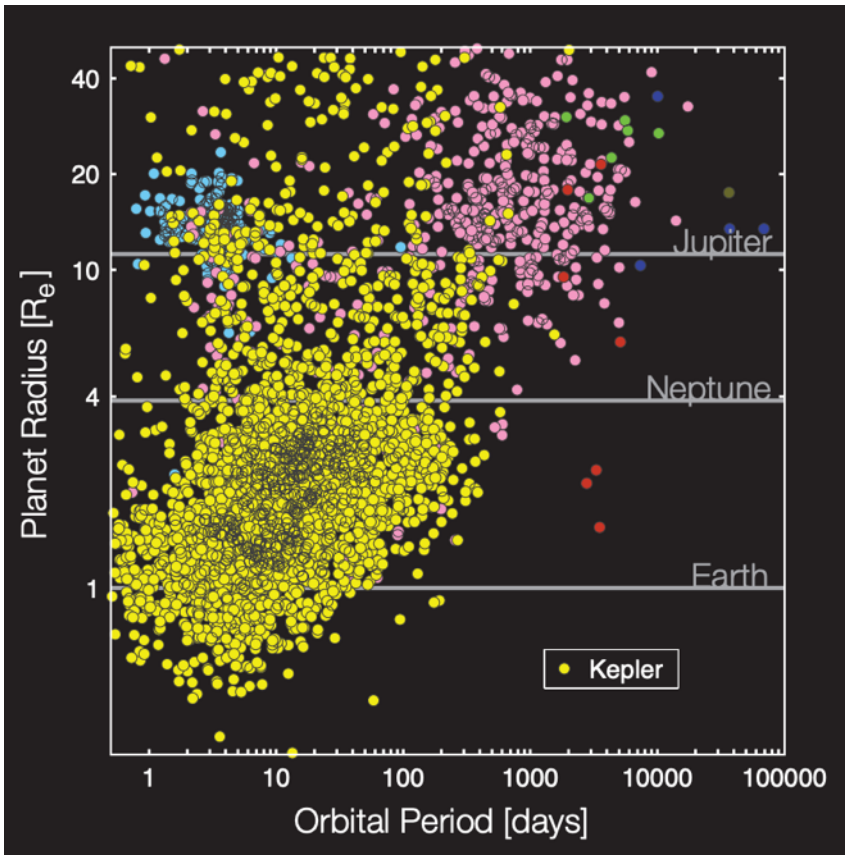

Figure 5.5 The observation of Kepler Telescope (Batalha, 2014).

The Kepler Space Telescope found that the largest population of exoplanets is Uranus / Neptune size or sub-Uranus / sub-Neptune size, as shown in Figure 5.5 [Batalha, 2014]. How the Uranus-like or Neptune-like magnetospheres protect the exoplanets from the stellar wind is very important in order to investigate the habitability of these worlds. As our multifluid MHD model is capable of simulating planetary global magnetospheres with any rotational and magnetic geometry, one of my plans for future work will be the application of our multifluid MHD model to the magnetospheres of exoplanets. Comparative studies between the magnetospheres of exoplanets with significantly different

orbital locations and stellar wind conditions and the planets in our solar system will help us understand deeply about the world where we live in and the other world beyond us.

REFERENCES

Arridge, C. S. (2015). Magnetotails of Uranus and Neptune. in *Magnetotails in the Solar System*, Vol. 207, edited by Andreas Keiling et al., pp. 119-133, American Geophysical Union, Washington, US.

Arridge, C. S., Achilleos, N., Dougherty, M. K., Khurana, K. K., & Russell, C. T. (2006). Modeling the size and shape of Saturn's magnetopause with variable dynamic pressure. *Journal of Geophysical Research: Space Physics*, 111(A11).

Arridge, C. S., Khurana, K. K., Russell, C. T., Southwood, D. J., Achilleos, N., Dougherty, M. K., ... & Leinweber, H. K. (2008). Warping of Saturn's magnetospheric and magnetotail current sheets. *Journal of Geophysical Research: Space Physics*, 113(A8).

Atreya, S. K., and T. M. Donahue (1975). Ionospheric models of Saturn, Uranus, and Neptune, *Icarus* 24(3), 358-362.

Bagenal, F., Belcher, J. W., Sittler, E. C., & Lepping, R. P. (1987). The Uranian bow shock: Voyager 2 inbound observations of a high Mach number shock. *Journal of Geophysical Research: Space Physics*, 92(A8), 8603-8612.

Batalha, N. M. (2014). Exploring exoplanet populations with NASA's Kepler Mission. *Proceedings of the National Academy of Sciences*, 111(35), 12647-12654.

Baumjohann, W., & Treumann, R. A. (1996). Basic space plasma physics, Imperial coll. Press, London.

Behannon, K. W., Lepping, R. P., Sittler, E. C., Ness, N. F., Mauk, B. H., Krimigis, S. M., & McNutt, R. L. (1987). The magnetotail of Uranus. *Journal of Geophysical Research: Space Physics*, 92(A13), 15354-15366.

Belcher, J. W., et al. (1991). The plasma environment of Uranus, *Uranus*, pp. 780–830, Univ. of Ariz. Press, Tucson.

Battey-Pratt, E. P., and Racey, T. J. (1980). Geometric model for fundamental particles. *International Journal of Theoretical Physics*, 19(6), 437-475.

Bridge, H. S. et al. (1986). Plasma observations near Uranus: Initial results from Voyager 2. *Science*, 233, 89-94.

Broadfoot, A. L., et al. (1986). Ultraviolet spectrometer observations of Uranus, *Science*, 233,74–79, doi:10.1126/science.233.4759.74.

Cao, X., & Paty, C. (2017). Diurnal and seasonal variability of Uranus's magnetosphere. *Journal of Geophysical Research: Space Physics*, 122(6), 6318-6331.

Cao, X., & Paty, C. (2014), A Seasonal Study of Uranus' Magnetosphere, *AGU fall meeting*, SM51E-4283

Cao, X., & Paty, C. (2015), 3D Multifluid MHD simulation for Uranus and Neptune: the seasonal variations of their magnetosphere, *AGU fall meeting*, SM31C-2503

Chandler, M. O., and Waite, J. H. (1986). The ionosphere of Uranus: A myriad of possibilities. *Geophysical research letters*, 13(1), 6-9.

Cnossen, I., & Richmond, A. D. (2012). How changes in the tilt angle of the geomagnetic dipole affect the coupled magnetosphere‐ionosphere‐thermosphere system. *Journal of Geophysical Research: Space Physics*, 117(A10).

Connerney, J. E. P. (1993). Magnetic fields of the outer planets. *Journal of Geophysical Research: Planets*, 98(E10), 18659-18679.

Cowley, S. W. H. (2013). Response of Uranus' auroras to solar wind compressions at equinox. *Journal of Geophysical Research: Space Physics*, 118(6), 2897-2902.

Desch, M. D., et al. (1986). The rotation period of Uranus, *Nature*, 322, 42–43, doi:10.1038/322042a0

Dong, C., Bougher, S. W., Ma, Y., Tóth, G., Nagy, A. F., & Najib, D. (2014). Solar wind interaction with Mars upper atmosphere: Results from the one-way coupling between the multifluid MHD model and the MTGCM model. *Geophysical Research Letters*, 41(8), 2708-2715.

Dungey, J. W. (1961). Interplanetary Magnetic Field and the Auroral Zones, *Physical Review Letters*, 6(2), 47-48.

Gurnett, D. A., Kurth, W. S., Scarf, F. L., and Poynter, R. L. (1986). First plasma wave observations of Uranus. *Science*, 233(4759), 106-109.

Hammond, C. M., Walker, R. J., & Kivelson, M. G. (1990). A Pincer‐shaped plasma sheet at Uranus. *Journal of Geophysical Research: Space Physics*, 95(A9), 14987-14994.

Herbert, F., and Sandel, B. R. (1994). The Uranian aurora and its relationship to the magnetosphere. *Journal of Geophysical Research: Space Physics*, 99(A3), 4143-4160.

Herbert, F. (2009). Aurora and magnetic field of Uranus, *Journal of Geophysical Research*, 114, A11206, doi:10.1029/2009JA014394.

Hofstadter, M. The case for a Uranus orbiter.

Korth, H., Anderson, B. J., Frey, H. U., and Waters, C. L. (2005). High-latitude electromagnetic and particle energy flux during an event with sustained strongly northward IMF. In *Annales geophysicae* (Vol. 23, No. 4, pp. 1295-1310).

Krimigis, S. M. et al. (1986). The magnetosphere of Uranus: Hot plasma and radiation environment. *Science*, 233, 97-103.

Kurth, W. S., Gurnett, D. A., Scarf, F. L., & Mauk, B. H. (1989). Plasma waves in the magnetotail of Uranus. *Journal of Geophysical Research: Space Physics*, 94(A4), 3505-3512.

Lam, H. A., et al. (1997). Variation in the H^3+ emission of Uranus, *Astrophys. J. Lett.*, 474, L73, doi:10.1086/310424.

Lamy, L. et al. (2012). Earth-based detection of Uranus' aurorae. *Geophysical Research Letters*, 39(7).

Lamy, L., Prangé, R., Hansen, K. C., Tao, C., Cowley, S. W. H., Stallard, T. S., ... & Kim, T. (2017). The aurorae of Uranus past equinox. *Journal of Geophysical Research: Space Physics*, 122(4), 3997-4008.

Lepping, R. P., T. A. Volliner, J. A. Jones, and N. F. Ness, (1989). Plots of Voyager2 Uranus magneticfield data, *report NASA Goddard SpaceFlight Cent.*, Greenbelt,MD.

Li, W., Knipp, D., Lei, J., and Raeder, J. (2011). The relation between dayside local Poynting flux enhancement and cusp reconnection. *Journal of Geophysical Research: Space Physics*, 116(A8).

Lin, R. L., Zhang, X. X., Liu, S. Q., Wang, Y. L., & Gong, J. C. (2010). A three‐dimensional asymmetric magnetopause model. *Journal of Geophysical Research: Space Physics*, 115(A4).

Lindal, G. F., Lyons, J. R., Sweetnam, D. N., Eshleman, V. R., Hinson, D. P., and Tyler, G. L. (1987). The atmosphere of Uranus: Results of radio occultation measurements with Voyager 2. *Journal of Geophysical Research: Space Physics*, 92(A13), 14987-15001.

Liu, Z. Q., Lu, J. Y., Kabin, K., Yang, Y. F., Zhao, M. X., and Cao, X. (2012). Dipole tilt control of the magnetopause for southward IMF from global magnetohydrodynamic simulations. *Journal of Geophysical Research: Space Physics*, 117(A7).

Lu, J. Y., Jing, H., Liu, Z. Q., Kabin, K., and Jiang, Y. (2013). Energy transfer across the magnetopause for northward and southward interplanetary magnetic fields. *Journal of Geophysical Research: Space Physics*, 118(5), 2021-2033.

Majeed, T., Waite, J. H., Bougher, S. W., Yelle, R. V., Gladstone, G. R., McConnell, J. C., and Bhardwaj, A. (2004). The ionospheres–thermospheres of the giant planets. *Advances in Space Research*, 33(2), 197-211.

Masters, A. (2014). Magnetic reconnection at Uranus' magnetopause. *Journal of Geophysical Research: Space Physics*, 119(7), 5520-5538.

Ma, X., Delamere, P., Otto, A., & Burkholder, B. (2017). Plasma transport driven by the three‐dimensional Kelvin‐Helmholtz instability. *Journal of Geophysical Research: Space Physics*, 122(10), 10-382.

Mejnertsen, L., Eastwood, J. P., Chittenden, J. P., & Masters, A. (2016). Global MHD simulations of Neptune's magnetosphere. *Journal of Geophysical Research: Space Physics*, 121(8), 7497-7513.

Melin, H., Stallard, T., Miller, S., Trafton, L. M., Encrenaz, T., and Geballe, T. R. (2011). Seasonal variability in the ionosphere of Uranus. *The Astrophysical Journal*, 729(2), 134.

Mosqueira, I., & Estrada, P. R. (2006). Jupiter's obliquity and a long-lived circumplanetary disk. *Icarus*, 180(1), 93-97.

NASA, (2010). NASA's 2010 science plan: For NASA's Science Mission Directorate

National Academy of Sciences, (2011). Vision and Voyages for Planetary Science in the Decade 2013-2022, The National Academies Press. Washington, D.C.

Ness, N. F. et al., (1986). Magnetic fields at Uranus. *Science*, 233, 85-90.

Palmroth, M., Pulkkinen, T. I., Janhunen, P., & Wu, C. C. (2003). Stormtime energy transfer in global MHD simulation. *Journal of Geophysical Research: Space Physics*, 108(A1).

Parker, E. N. (1958). Dynamics of the interplanetary gas and magnetic fields. *The Astrophysical Journal*, 128, 664.

Paty, C., and Winglee, R. (2004). Multi-fluid simulations of Ganymede's magnetosphere. *Geophysical research letters*, 31(24).

Paty, C., and Winglee, R. (2006). The role of ion cyclotron motion at Ganymede: Magnetic field morphology and magnetospheric dynamics. *Geophysical research letters*, 33(10).

Paty, C. and Cao, X. (2018). The magnetospheric interaction between Neptune and Triton. *Conference on Magnetospheres of the Outer Planets*.

Richard S, et al., (1987). Voyager 2 plasma ion observations in the magnetosphere of Uranus, *Journal of Geophysical Research*, VOL. 92, NO. A13, 15,249-15,262

Russell, C. T. (1993). "Planetary magnetospheres". *Rep. Prog. Phys*. (56): 687-732

Russell, C. T., & Dougherty, M. K. (2010). Magnetic fields of the outer planets. *Space science reviews*, 152(1-4), 251-269.

Schulz, M., and McNab, M. C. (1996). Source-surface modeling of planetary magnetospheres. *Journal of Geophysical Research: Space Physics*, 101(A3), 5095-5118.

Shue, J. H., Chao, J. K., Fu, H. C., Russell, C. T., Song, P., Khurana, K. K., & Singer, H. J. (1997). A new functional form to study the solar wind control of the magnetopause size and shape. *Journal of Geophysical Research: Space Physics*, 102(A5), 9497-9511.

Shue, J. H., Song, P., Russell, C. T., Steinberg, J. T., Chao, J. K., Zastenker, G., ... & Kawano, H. (1998). Magnetopause location under extreme solar wind conditions. *Journal of Geophysical Research: Space Physics*, 103(A8), 17691-17700.

Tóth, G., Kovács, D., Hansen, K. C., and Gombosi, T. I. (2004). Three-dimensional MHD simulations of the magnetosphere of Uranus. *Journal of Geophysical Research: Space Physics*, 109(A11).

Trafton, L. M., et al. (1999). H_2 Quadrupole and H_3^+ emission from Uranus: The Uranian thermosphere, ionosphere, and aurora, *Astrophys. J.*, 524, 1059–1083, doi:10.1086/307838.

Vasyliunas, V. M. (1983). Plasma distribution and flow, in Physics of the Jovian Magnetosphere , edited by A. J. Dessler, pp. 395–453, Cambridge Univ. Press, Cambridge, U. K.

Vasyliunas, V. M. (1986). The convection-dominated magnetosphere of Uranus. *Geophysical research letters*, 13(7), 621-623..

Voight, G. H., Hill, T. W., and Dessler, A. J. (1983). The magnetosphere of Uranus-Plasma sources, convection, and field configuration. *The Astrophysical Journal*, 266, 390-401.

Voigt, G. H., Behannon, K. W., and Ness, N. F. (1987). Magnetic field and current structures in the magnetosphere of Uranus. *Journal of Geophysical Research: Space Physics*, 92(A13), 15337-15346.

Waite, J. H., and Cravens, T. E. (1987). Current review of the Jupiter, Saturn, and Uranus ionospheres. *Advances in space research*, 7(12), 119-134.

Walker, R. J., Ogino, T., & Ashour‐Abdalla, M. (1989). Simulating the magnetosphere: The structure of the magnetotail. *Solar System Plasma Physics*, 54, 61-68.

Winglee, R. M. (1998). Multi-fluid simulations of the magnetosphere: The identification of the geopause and its variation with IMF. *Geophysical research letters*, 25(24), 4441-4444.

Winglee, R. M., Snowden, D., & Kidder, A. (2009). Modification of Titan's ion tail and the Kronian magnetosphere: Coupled magnetospheric simulations. *Journal of Geophysical Research: Space Physics*, 114(A5).

Winslow, R. M., Anderson, B. J., Johnson, C. L., Slavin, J. A., Korth, H., Purucker, M. E., ... & Solomon, S. C. (2013). Mercury's magnetopause and bow shock from MESSENGER Magnetometer observations. *Journal of Geophysical Research: Space Physics*, 118(5), 2213-2227.

Winslow, R. M., Philpott, L., Paty, C. S., Lugaz, N., Schwadron, N. A., Johnson, C. L., & Korth, H. (2017). Statistical study of ICME effects on Mercury's magnetospheric boundaries and northern cusp region from MESSENGER. *Journal of Geophysical Research: Space Physics*, 122(5), 4960-4975.

Xue, S., Cairns, I. H., Smith, C. W., and Gurnett, D. A. (1996). A Study of Uranus' bow shock motions using Langmuir waves. *Journal of Geophysical Research*, 101, 7659-7676.

Ye, G., & Hill, T. W. (1994). Solar-wind-driven convection in the Uranian magnetosphere. *Journal of Geophysical Research: Space Physics*, 99(A9), 17225-17235.

Zhang, Q. H., Lockwood, M., Foster, J. C., Zhang, S. R., Zhang, B. C., McCrea, I. W., ... & Ruohoniemi, J. M. (2015). Direct observations of the full Dungey convection cycle in the polar ionosphere for southward interplanetary magnetic field conditions. *Journal of Geophysical Research: Space Physics*, 120(6), 4519-4530.